

MODIFICATION OF INTRINSIC REFRACTIVE INDEX OPTICAL FIBER
SENSOR VIA PRECISE CLADDING REMOVAL AND HETEROGENEOUS
ZnO/Ag BI-LAYER COATING

ZAHRA SAMAVATI

UNIVERSITI TEKNOLOGI MALAYSIA

MODIFICATION OF INTRINSIC REFRACTIVE INDEX OPTICAL FIBER
SENSOR VIA PRECISE CLADDING REMOVAL AND HETEROGENEOUS
ZnO/Ag BI-LAYER COATING

ZAHRA SAMAVATI

A thesis submitted in fulfilment of the
requirements for the award of the degree of
Doctor of Philosophy

School of Chemical and Energy Engineering
Faculty of Engineering
Universiti of Teknologi Malaysia

SEPTEMBER 2020

DEDICATION

In the Name of Allah, the Most Merciful, the Most Compassionate all praise be to Allah, the Lord of the worlds. First and foremost, I must acknowledge my limitless thanks to Allah, the Ever-Magnificent; the Ever-Thankful, for His helps and bless. I am totally sure that this work would have never become truth, without His guidance. I dedicate my dissertation work to my family and my friends. A special feeling of gratitude to my loving parents (Ahmad and Hamideh) whose words of encouragement and push for tenacity ring in my ears and beloved brother (Alireza) who was like my backbone and still supports me virtually. He was the only reason for my current position. His love and dedication to the upliftment in my life is incredible. I pay homage to my brother. I am also dedicating this dissertation to my many friends who have supported me throughout the process. I will always appreciate all they have done, especially Mohamad Aizat Abu Bakar, Koo KhongNee, Dayang Norafizan Binti Awang Chee, Samuel Ansong and Vahid Khosravi.

ACKNOWLEDGEMENT

I would first express my deep, heartfelt gratitude and reverence to my research supervisor Prof. Datuk. Ts. Dr. Ahmad Fauzi Bin Ismail, for his guidance, advice, support and encouragement during my research. His affection and support in all aspects have made me to complete the thesis successfully. On the other hand, would like to thank my co-supervisors Prof. Dr. Noorhana Yahya and Assoc. Prof. Dr. Mukhlis A Rahman for providing me moral support, help and encouragement throughout the period of this research. Also, it is my pleasure to thank Registrar, Assoc. Prof. Ts. Dr. Mohd Hafiz Dzarfan Othman for his invaluable help in administrative matters and support in every aspect of the completion of my research work. I would like to take this opportunity to say warm thanks to Dr Alireza Samavati for his valuable advice and generous support during my research work.

ABSTRACT

Miniaturized refractive index sensor by combination of nanostructure thin films as a transformer sensitive layer and optical fiber as a signal carrier offers great potential for identifying the environmental features and understanding the novel sensor concepts. The partially unclad and bi-layer zinc oxide (ZnO) / silver (Ag) coated multimode glass and polymer optical fiber as a simple and reliable intrinsic fiber sensor was proposed in this work to detect the ambient refractive index changes (saline and crude oil having various concentrations) using two broadband sources of infrared radiation and ultraviolet-visible. The removing process to partially unclad the polymer and glass fiber was carried out precisely using our proposed dynamic monitoring process to prevent any interruption on propagating light by occurrence of damage on the core surface. The ZnO as an outer sensitive layer had three configuration which was spherical nanoparticle, horizontally and vertically oriented nanorods deposited on discontinuous Ag layer using mixture of electroless, dip coating and low temperature hydrothermal techniques because solo deposition technique was not possible. Ag nano-island shape deposition made the transition of evanescent wave to external media possibly through this semi-reflectance structure. ZnO coating avoided the formation of oxygen deficit defects, inhibited aging problem and trapping measurand molecules through mechanical interlock phenomena which altered its optical characteristics and improved sensitivity of the sensor. The x-ray diffraction spectra demonstrate that the level of crystallinity was higher for vertically oriented ZnO compared to others. Using field emission scanning electron microscope images, the width/length of vertically and horizontally oriented ZnO nanorods was measured to be ~ 86 nm/ ~ 690 nm and ~ 67 nm/ ~ 544 nm, respectively. The ZnO nanoparticle size was in the range of ~ 10 nm to ~ 75 nm. Surface roughness of ZnO/Ag coated glass (polymer) probe extracted from atomic force microscopy was ~ 39 (52 nm), ~ 52 (176 nm) and ~ 148 (346 nm) for nanoparticles, horizontally and vertically nanorods respectively. Room temperature Photoluminescence spectra from bi-layer ZnO/Ag coated on glass substrate when contacted with saline and crude oil having different concentrations revealed that near band edge emission band gap shifted from ~ 3.447 eV to ~ 3.189 eV going from sphere nanoparticles to vertically oriented nanorods. This shift is independent with the contact media. However, deep level emission depends strongly on the concentration of the contacted media. The shift observed for nanoparticle, horizontally and vertically oriented ZnO/Ag when contacted with saline (crude oil) was ~ 0.05 eV (~ 0.09 eV), ~ 0.02 eV (~ 0.03 eV) and ~ 0.08 eV (~ 0.11 eV) respectively. The performance of fabricated probe to detect saline concentration changes for glass fiber coated with vertically oriented ZnO nanorods/Ag when IR light source employed, was supreme compared to the other samples and was reported to be 255.4 nm/RIU and 314.2 dB/RIU for wavelength and intensity sensing respectively. The durable polymer fiber coated with vertically oriented ZnO/Ag nanorods showed the intensity and wavelength sensitivity of 146.2 dB/RIU and 78.5nm/RIU respectively in identifying the variation of crude oil from 0 to 100%. The optimum length of glass and polymer fiber probe for maximum sensitivity was obtained for 3 cm and 2 cm respectively. The precise production techniques together with comprehensive analysis of the sensing mechanism lead to a deeper understanding of the liquid refractive index behavior applicable in quality control in water resource and oil reservoir.

ABSTRAK

Penderia indeks biasan miniatur dengan gabungan filem nipis nanostruktur sebagai lapisan sensitif pengubah dan gentian optik sebagai pembawa isyarat berpotensi untuk mengenal pasti keadaan sekeliling dan memahami konsep penderia baharu. Gentian optik kaca dan polimer berbilang mod yang telah dinyahsalut sebahagiannya dan disalut dengan dwilapisan zink oksida (ZnO) / perak (Ag) bertindak sebagai penderia gentian intrinsik yang mudah dan boleh dipercayai dicadangkan untuk mengesan perubahan indeks biasan (air garam dan minyak mentah pada pelbagai kepekatan) dengan menggunakan dua sumber jalur lebar, inframerah dan ultraungu-cahaya tampak. Proses penyahsalutan separa gentian polimer dan kaca secara terperinci dilakukan dengan pemantauan secara dinamik seperti yang dicadangkan untuk mengelakkan sebarang gangguan terhadap penyebaran cahaya melalui kerosakan pada permukaan teras gentian optik. ZnO sebagai lapisan sensitif luaran mempunyai tiga konfigurasi iaitu nanopartikel sfera, nanorod berorientasi mendatar dan menegak, endapan pada lapisan Ag yang berlainan menggunakan campuran elektroless, salutan celupan dan teknik hidrotermal suhu rendah kerana teknik endapan tidak dapat dilakukan secara solo. Endapan nano-pulau Ag menjadikan peralihan gelombang sisihan ke media luaran terhasil melalui struktur pemantulan separa ini. Salutan ZnO mengelakkan pembentukan kerosakan defisit oksigen, merencat masalah penuaan dan memerangkap molekul ukuran melalui fenomena interlok mekanikal yang mengubah percirian optik dan meningkatkan sensitiviti penderia. Spektrum pembelauan sinar-X menunjukkan bahawa tahap pengkristalan ZnO yang berorientasi tegak lebih tinggi berbanding yang lain. Melalui imej mikroskop imbasan elektron pancaran medan, lebar / panjang nanorod ZnO yang berorientasikan secara menegak dan melintang diukur masing-masing sebanyak ~ 86 nm / ~ 690 nm dan ~ 67 nm / ~ 544 nm. Saiz nanopartikel ZnO ialah dalam julat ~ 10 nm hingga ~ 75 nm. Kekasaran permukaan kuar kaca (polimer) bersalut ZnO / Ag yang diekstrak dari mikroskop daya atom masing-masing adalah ~ 39 (52 nm), ~ 52 (176 nm) dan ~ 148 (346 nm) untuk nanopartikel, secara mendatar dan menegak. Spektrum foto pendarcahaya pada suhu bilik dari lapisan ZnO / Ag bersalut pada substrat kaca apabila bersentuhan dengan larutan garam dan minyak mentah yang berbeza kepekatan menunjukkan peralihan hampir jalur pinggir ~ 3.447 eV ke ~ 3.189 eV nanopartikel sfera ke arah nanorod berorientasi tegak. Peralihan ini tidak dipengaruhi oleh media sentuhan. Walau bagaimanapun, pelepasan paras dalam sangat bergantung kepada kepekatan media yang bersentuhan. Peralihan yang diperhatikan untuk nanopartikel, ZnO / Ag berorientasikan secara mendatar dan menegak apabila berinteraksi dengan larutan garam (minyak mentah) masing-masing adalah ~ 0.05 eV (~ 0.09 eV), ~ 0.02 eV (~ 0.03 eV) dan ~ 0.08 eV (~ 0.11 eV). Prestasi kuar yang difabrikasi untuk mengesan perubahan kepekatan garam untuk gentian kaca yang dilapisi dengan nanorod berorientasikan ZnO / Ag menegak ketika sumber cahaya IR digunakan, dibandingkan dengan sampel yang lain dan dilaporkan masing-masing sebanyak 255.4 nm / RIU dan 314.2 dB / RIU untuk panjang gelombang dan intensiti. Polimer tahan lasak yang bersalut dengan nanorod ZnO / Ag berorientasikan menegak menunjukkan sensitiviti intensiti dan panjang gelombang sebanyak masing-masing 146.2 dB / RIU dan 78.5 nm / RIU untuk mengenal pasti kepekatan minyak mentah dari 0% hingga 100%. Panjang optimum kuar gentian kaca dan polimer untuk sensitiviti maksimum adalah masing-masing pada 3 cm dan 2 cm. Teknik pembuatan yang teliti berserta dengan analisis yang komprehensif membawa kepada kefahaman yang lebih mendalam terhadap keadaan serakan indeks cecair yang mana mampu menyumbang kepada kawalan mutu sumber air dan takungan minyak.

TABLE OF CONTENTS

	TITLE	PAGE
	DECLARATION	ii
	DEDICATION	iii
	ACKNOWLEDGEMENT	iv
	ABSTRACT	v
	ABSTRAK	vi
	TABLE OF CONTENTS	vii
	LIST OF TABLES	x
	LIST OF FIGURES	xii
	LIST OF ABBREVIATIONS	xvii
	LIST OF SYMBOLS	xix
	LIST OF APPENDICES	xxii
CHAPTER 1	INTRODUCTION	1
	1.1 Research Background	1
	1.2 Statement of the Problems	2
	1.3 Objectives of the Study	4
	1.4 Scopes of the Research	5
	1.5 Significance of Study	7
	1.6 Organization of Thesis	8
CHAPTER 2	LETRATURE REVIEW	10
	2.1 Introduction	10
	2.2 Optical Fiber Principles and Applications	12
	2.3 Optical Fiber Category	14
	2.3.1 Optical Fibers Based on Fabricated Material	14
	2.3.2 Optical Fiber Based on Propagation Mode	15
	2.3.3 Optical Fibers Based on Refractive Index	17
	2.4 Optical Fiber Sensors	18

2.4.1	Optical Fiber Sensor Classification	19
2.4.1.1	Intrinsic and Extrinsic	19
2.4.2	Intensity and Wavelength Modulated Optical Fiber Sensor	22
2.4.3	Sensing Mechanism	26
2.4.3.1	Intensity Changes as a Sensing Element	26
2.4.3.2	Wavelength Modulated as a Sensing Element	29
2.5	Fabricated Optical Fiber Sensor	31
2.5.1	Unclad Optical Fiber Sensor	31
2.5.2	Coated Unclad Optical Fiber Sensor	35
2.5.2.1	Coated Sensitive Materials	35
2.5.2.2	Coating Techniques	45
2.6	Review of Coated Optical Fiber Probe with Ag, ZnO and Their Hybrid Component	53
2.7	Saline and crude oil as an analyte media	56
CHAPTER 3	RESEARCH METHODOLOGY	58
3.1	Introduction	58
3.2	Materials Selection	61
3.3	Partially-unclad Process	63
3.4	Coating Fiber with Ag and ZnO Nanostructures	64
3.5	Experimental Setup and Characterization of the Probe	68
3.6	Characterization Techniques	70
CHAPTER 4	RESULTS AND DISCUSSION	75
4.1	Introduction	75
4.2	Partially-unclad Optical Fiber Sensor	77
4.2.1	Morphology of Partially-unclad Sensor	79
4.2.2	Performance of Partially-unclad Probe	85
4.2.2.1	Effect of Probe Length	87
4.2.2.2	Effect of Solution Concentration	89
4.3	ZnO/Ag Coated Partially-unclad Optical Fiber Sensor	93

4.3.1	Morphology and Structure of the ZnO/Ag/Fiber Probe	93
4.4	Surface Charge Study and Optical Characteristics of Bi-layer ZnO/Ag	110
4.4.1	Optical and Surface Charge Behavior of ZnO/Ag Interact with Saline	110
4.4.2	Optical Behavior of ZnO/Ag Interact with Crude oil	118
4.4.3	Transmittance Analysis for ZnO/Ag	123
4.5	Performance of ZnO/Ag Bi-layer Coated on Partially-unclad Optical Fiber Probe	125
4.5.1	Probe Performance Test on Both GOF and POF Sensors	126
4.5.2	Length Dependent Sensitivity of ZnO (NRV) / Ag / GFiber and ZnO (NRV) / Ag / PFiber	141
4.5.3	Tensile Analysis of ZnO (NRV)/Ag/GOF and ZnO (NRV)/Ag/POF	144
CHAPTER 5	CONCLUSION AND RECOMMENDATIONS	146
5.1	Achievements of the Study	146
5.2	Research Limitations	149
5.3	Future Works	150
REFERENCES		151
LIST OF PUBLICATIONS		174

LIST OF TABLES

TABLE NO.	TITLE	PAGE
Table 2.1	Advantages of multimode and single mode optical fiber	16
Table 2.2	Step index and graded index optical fiber	18
Table 2.3	Characteristics of extrinsic and intrinsic fiber optic sensor	21
Table 2.4	Etching parameters for removing the glass optical fiber cladding	33
Table 2.5	Etching parameters for removing the polymer optical fiber cladding	34
Table 2.6	Optoelectronic features of Ag, Au and Cu coated on insulator substrate	38
Table 2.7	Positive and negative aspects of physical and chemical deposition techniques	47
Table 2.8	Recent study on optical fiber probe coated with Ag and ZnO	54
Table 3.1	List of chemical materials to fabricate optical fiber sensors	61
Table 3.2	Crude oil characteristics	62
Table 3.3	The summary of fabricated samples	68
Table 4.1	Sensitivity of the GOF and POF probe as a function of sensing length	88
Table 4.2	Roughness, absorption coefficient and sensitivity of the GOF sensors as a function of HF concentration	92
Table 4.3	Roughness, absorption coefficient and sensitivity of the POF sensors as a function of acetone/methanol concentration	92
Table 4.4	Contact angle of saline-probe surface and crude oil-probe surface	109
Table 4.5	The light absorption value at different saline concentration	117
Table 4.6	The light absorption value at different crude oil concentration	122

Table 4.7	Sensitivity against saline concentration	129
Table 4.8	Sensitivity against crude oil concentration	133
Table 4.9	Sensitivity against saline concentration at three propagating main modes	137
Table 4.10	Sensitivity against crude oil concentration at three propagating main modes	140
Table 4.11	Sensitivity of ZnO (NRV) / Ag/ GOF and ZnO (NRV) / Ag / POF against sensing length	144

LIST OF FIGURES

FIGURE NO.	TITLE	PAGE
Figure 2.1	Map of literature review	11
Figure 2.2	Structure of optical fiber	12
Figure 2.3	Light behaviors at the interface of two transparent medium	13
Figure 2.4	Classification of optical fiber	14
Figure 2.5	Schematic diagram of single and multimode fiber	16
Figure 2.6	(a) Step-index and (b) graded-index fiber	17
Figure 2.7	Extrinsic optical sensor	20
Figure 2.8	Intrinsic optical sensor	20
Figure 2.9	Classification of intrinsic fiber optics sensor	21
Figure 2.10	Schematic diagram of the evanescent wave	23
Figure 2.11	The schematic diagram of the light transition in partially unclad optical fiber	28
Figure 2.12	Schematic diagrams of (a) tapered fiber and (b) partially unclad fiber	32
Figure 2.13	SPR in the interface of metal-insulator material in optical fiber sensor	36
Figure 2.14	Schematic diagram of modifying the ZnO band gap by contacting with media.	44
Figure 2.15	Refractive index of the ZnO as a function of energy gap	45
Figure 2.16	Physical and chemical deposition techniques	46
Figure 2.17	Flowchart of processing steps for electroless method	50
Figure 2.18	Deposition process of Ag with electroless method	51
Figure 2.19	Schematic diagram of ZnO/Fiber deposition process	52
Figure 3.1	Flowchart of the experimental procedure	60
Figure 3.2	Experimental setup for real-time power monitoring	64
Figure 3.3	Steps for Ag deposition and its corresponding real image	65
Figure 3.4	Experimental set-up for refractive index sensing	70
Figure 4.1	Flowchart for results and discussion	77
Figure 4.2	The dynamic power transmission at different solvent concentration	78

Figure 4.3	Top-view FESEM images of the fiber sensor prepared at (a) 20%, (b) 25 %, (c) 30 % and (d) 35 % HF concentration	79
Figure 4.4	Mechanism of silica glass, etching at (a) 20 %, (b) 25 %, (c) 30 % and (d) 35 % of HF concentration	80
Figure 4.5	Top-view AFM images of glass fiber probe etched at (a) 20 %, (b) 25%, (c) 30 % and (d) 35 % HF. Inset shows the line scan profile	81
Figure 4.6	Top-view FESEM images of the fiber sensor prepared at acetone/methanol having percentages of (a) 50/50, (b) 40/60, (c) 30/70 and (d) 20/80	82
Figure 4.7	Schematic of acetone/methanol etching mechanism to remove cladding and its corresponding real images	83
Figure 4.8	3D AFM images of partially removed polymer fiber using acetone/methanol concentration of (a) 50/50, (b) 40/60, (c) 30/70 and (d) 20/80	84
Figure 4.9	(a) The dynamic intensity changes as a function of etching time at different temperature, (b) proposed step-reducing the etching temperature. Inset: FESEM image of cladding after 57 min etching time	86
Figure 4.10	The dynamic intensity changes as a function of etching time using (a) 40/60(acetone/methanol) solutions in different temperature, (b) FESEM image after 423 sec in 15°C etching	87
Figure 4.11	Probe length dependent sensitivity of the partially unclad glass and polymer fiber sensor	88
Figure 4.12	Intensity variation for sensors prepared at variety of HF concentration when expose to (a) saline and (b) crude oil with different refractive index	90
Figure 4.13	Intensity variation for sensors prepared at variety of acetone/methanol concentration when expose to (a) saline and (b) crude oil with different refractive index	90
Figure 4.14	(a) FESEM images of surface view and (b) cross section of Ag nanoparticles coated on glass fiber	94
Figure 4.15	(a) EDX mapping and spectra of selected area on the Ag/GFiber surface and (b) cross section	95
Figure 4.16	(a, b) FESEM images of surface view and (c) cross section of Ag nanoparticles coated on polymer fiber	96
Figure 4.17	(a) EDX mapping and spectra of a particular selected area on the Ag/POF surface and (b) cross section	97

Figure 4.18	FESEM images of (a-b) ZnO(NPs)/Ag/GFiber, (c-d) ZnO(NRH)/Ag/ GFiber and (e-f) ZnO(NRV)/Ag/ GFiber. Inset: Corresponding EDX spectra and mapping	99
Figure 4.19	Size distribution diagram of ZnO (a) nanoparticles, (b, c) horizontally, and (d, e) vertically oriented nanorods	100
Figure 4.20	X-ray diffraction pattern of ZnO nanostructures deposited on Ag/glass substrate	101
Figure 4.21	3D AFM images of ZnO (a) nanoparticles, (b) horizontal, and (c) vertical nanorods deposited on Ag/GFiber	102
Figure 4.22	Cross section FESEM, EDX spectra and elemental mapping of (a, b) ZnO(NPs)/Ag/PFiber, (c, d) ZnO(NRH)/Ag/PFiber and (e, f) ZnO(NRV)/Ag/PFiber samples. Inset: top view FESEM images	103
Figure 4.23	The ZnO nanostructure size distribution determined with ImageJ software. (a) nanoparticles, (b, c) horizontally, and (d, e) vertically oriented nanorods	104
Figure 4.24	XRD patterns of ZnO nanostructures deposited on Ag/polymer substrate	105
Figure 4.25	3D AFM images of ZnO (a) nanoparticles, (b) horizontal and (c) vertical nanorods deposited on Ag/PFiber	106
Figure 4.26	Contact angle on (a) ideal smooth and (b) rough surface	107
Figure 4.27	(a) Saline and (b) crude oil contact angle with ZnO nanoparticles, horizontally and vertically aligned nanorods at 25°C	108
Figure 4.28	Ag/ZnO deposited on glass substrate	110
Figure 4.29	(a) Zeta potential ZnO nanostructures deposited on Ag/glass substrate against saline concentration. (b) Real condition sample preparation for ZP analysis	112
Figure 4.30	Schematic diagram of shape dependent charge distribution on ZnO nanostructure surface	112
Figure 4.31	Photoluminescence (PL) emission spectra for ZnO (a) nanoparticles, (b) horizontal and (c) vertical nanorods deposited on Ag/glass substrate immersed in saline	115
Figure 4.32	Room temperature absorbance spectra of different saline concentrations at (a) visible, and (b) NIR	117
Figure 4.33	Photoluminescence spectra of (a) ZnO nanoparticles, (b) horizontally and (c) vertically aligned nanorods deposited on Ag/glass substrate immersed in crude oil	121
Figure 4.34	Room temperature absorbance spectra as a function of crude oil concentration, at (a) visible and (b) NIR range	122

Figure 4.35	Light behavior at interfaces of core-cladding and cladding-nanolayer	123
Figure 4.36	The transmission spectra of samples. Inset depicts the discontinuous coated Ag nanoparticles on glass substrate	125
Figure 4.37	Transmission spectra of the (a) ZnO(NPs)/Ag/GFiber, (b) ZnO(NRH)/Ag/GFiber (c) ZnO(NRV)/Ag/GFiber probe once using visible light source as a function of saline concentration	127
Figure 4.38	Transmission spectra when IR light propagate through the probe of sample (a) ZnO(NPs)/Ag/GFiber, (b) ZnO(NRH)/Ag/GFiber (c) ZnO(NRV)/Ag/GFiber as a function of saline concentration	128
Figure 4.39	Wavelength and intensity modulation when visible and IR light source is used at different saline concentrations	129
Figure 4.40	Transmission spectra of visible light for sample (a) ZnO(NPs)/Ag/GFiber, (b) ZnO(NRH)/Ag/GFiber and (c) ZnO(NRV)/Ag/GFiber as a function of crude oil concentration	131
Figure 4.41	Transmission spectra of the (a) ZnO(NPs)/Ag/GFiber, (b) ZnO(NRH)/Ag/GFiber (c) ZnO(NRV)/Ag/GFiber probe once using IR light source	132
Figure 4.42	Wavelength and intensity modulation when visible and IR light source is used at different crude oil concentrations	133
Figure 4.43	Transmission spectra of the (a) ZnO(NPs)/Ag/PFiber, (b) ZnO(NRH)/Ag/ PFiber (c) ZnO(NRV)/Ag/ PFiber probe as a function of saline concentration. Inset: Gaussian fit centered at 770 nm	136
Figure 4.44	The (a) wavelength and (b) intensity changes of samples at three main propagating modes	136
Figure 4.45	The (a) wavelength and (b) intensity changes as a function of refractive index at 1072 nm wavelength for all samples	137
Figure 4.46	Transmission spectra of the (a) ZnO(NPs)/Ag/POF, (b) ZnO(NRH)/Ag/POF (c) ZnO(NRV)/Ag/POF as a function of crude oil concentration. Inset: Gaussian fit at 770 nm	139
Figure 4.47	Intensity and wavelength changes as a function of ZnO shape at 770 nm, 940 nm and 1072 nm	139
Figure 4.48	The intensity and wavelength changes as a function of crude oil RI at 1072 nm	140

Figure 4.49	Schematic diagram of ZnO shape dependence surface interaction with (a) saline and (b) crude oil molecules	141
Figure 4.50	Probe length dependent sensitivity of the ZnO(NRV)/Ag/GOF against (a, b) saline, and (c, d) crude oil	142
Figure 4.51	Probe length dependent sensitivity of the ZnO(NRV)/Ag/POF against (a, b) saline, and (c, d) crude oil	143
Figure 4.52	Strain versus force experimental data for (a) ZnO(NRV)/Ag/GOF and (b) ZnO(NRV)/Ag/POF	145

LIST OF ABBREVIATIONS

AFM	-	Atomic Force Microscopy
ALD	-	Atomic Layer Deposition
CEI	-	Cladding Environment Interface
CVD	-	Chemical Vapor Deposition
DC	-	Direct Current sputtering
DI	-	Distilled Water
DL	-	Deep-Level
EDX	-	Energy Dispersive X-ray Spectroscopy
EMI	-	Electro Magnetic Interference
Eq	-	Equation
EW	-	Evanescent Wave
Exp	-	Experimental
FBG	-	Fiber Bragg Grating
FESEM	-	Field Emission Scanning Electron Microscopy
FWHM	-	Full Width at Half Maximum
SG	-	Specific Gravity
IEA	-	International Energy Agency
USGS	-	US geological survey
GFiber	-	Glass Fiber
GOF	-	Glass Optical Fiber
HOMO	-	Highest Occupied Molecular Orbital
JCPDS	-	Joint Committee on Powder Diffraction Standards
LUMO	-	Lowest Unoccupied Molecular Orbital
LPG	-	Long Period Grating
LSP	-	Localized Surface Plasmon
LSPR	-	Localized Surface Plasmon Resonance
LSPRs	-	Localized Surface Plasmon Resonance Sensor
MBE	-	Molecular Beam Epitaxy
MOCVD	-	Metal Organic Chemical Vapour Deposition
NBE	-	Near Band Edge

NPs	-	Nanoparticles
NRH	-	Nanorods Horizontally
NRV	-	Nanorods Vertically
OSA	-	Optical Spectrum Analyzer
PC	-	Poly Carbonate
PVD	-	Physical Vapor Deposition
PECVD	-	Plasma Enhanced Chemical Vapour Deposition
PFiber	-	Polymer Fiber
PL	-	Photoluminescence
PMMA	-	Poly (methyl methacrylate)
POF	-	Plastic Optical Fiber
PS	-	Poly Styrene
RF	-	Radio Frequency Sputtering
RI	-	Refractive Index
RT	-	Room Temperature
SEM	-	Scanning Electron Microscopy
SPR	-	Surface Plasmon Resonance
TEM	-	Transverse Electro Magnetic
Theo	-	Theory
TIR	-	Total Internal Reflection
UV-VIS/NIR	-	Ultraviolet-Visible/Near Infrared
XRD	-	X-Ray powder Diffraction
ZP	-	Zeta Potential

LIST OF SYMBOLS

μm	-	Micrometer
nm	-	Nanometer
dBm	-	Decibel-milliwatts
mW	-	Milliwatts
mA	-	Milliampere
eV	-	Electron volt
mV	-	Millivolt
ppm	-	Parts-per-million
cm	-	Centimeter
min	-	Minute
$^{\circ}\text{C}$	-	Celsius degree
W/V	-	Weight per volume
V/V	-	Volume per volume
RH	-	Relative humidity
E	-	Evanescent field
d_p	-	Penetration depth
θ	-	Incident angle of light
λ	-	Wavelength
λ_0	-	Wavelength of incident light
dp	-	Penetration depth of the evanescent field
n	-	Refractive index
λ_B	-	Bragg grating wavelength
θ	-	Angle of incidence normal at the interface
n_{eff}	-	The effective refractive index of the fiber core
E_{Total}	-	Total cohesive energy
E_0	-	Cohesive energy of the bulk material
N	-	Number of surface atoms
A	-	Avogadro's number
σ_0	-	Pre-exponential constant
E_c	-	Energy of conduction band

E_F	-	Fermi energy
T_{mn}	-	Melting temperature of nanosize materials
T_{mb}	-	Melting temperature of bulk materials
ΔE_g	-	Energy bandgap variance
D	-	Diameter of spherical nanoparticle
l	-	Diameter of nanorod
ξ	-	Absorption coefficient
R_r	-	Roughness
D_i	-	Local diameter
h_i	-	Local depth
rf	-	Radio frequency
dc	-	Direct current
φ	-	Phase difference
ε	-	Dielectric constant
K_{sp}	-	Propagating constant of the surface plasmon
K_{eo}	-	Propagating constant of the evanescent wave
α	-	Absorption coefficient
ω	-	Angular frequency
Q_{SPR}	-	Quality factor surface plasmon resonance
I	-	Intensity
α	-	Absorption coefficient
t	-	Film thickness
D	-	Domain size
β	-	Full width
γ	-	Evanescent absorption coefficient
P	-	Power transmitted
ρ	-	Core radius
N	-	Total number of nanoparticles
Ag	-	Silver
$Ag\ NPs$	-	Silver nanoparticles
$Au\ NPs$	-	Gold nanoparticles
ZnO	-	Zinc oxide
Co	-	Cobalt

N_2	-	Nitrogen
HF	-	Hydrofluoric acid
Pd	-	Palladium
NaCl	-	Sodium chloride
GO-ZnO	-	Zinc oxide nanoparticle incorporated grapheme oxide
Ni	-	Nickel
$AgNO_3$	-	Silver nitrate
NH_3	-	Ammonia solution
NaOH	-	Sodium hydroxide
$Zn(NO_3)_2 \cdot 6H_2O$	-	Zinc Nitrate hexahydrate
$SnCl_2$	-	Tin (II) chloride
$PdCl_2$	-	Palladium (II) chloride
$(CH_3)_2NHBH_3$	-	Boron hydride dimethylamine
HCl	-	Hydrochloric acid
H_2SO_4	-	Sulfuric acid
Ge	-	Germanium
GeO_2	-	Germanium dioxide
P_2O_5	-	Phosphorus pentoxide
F	-	Fluorine
B_2O_3	-	Boron trioxide
O	-	Oxygen molecule
Si	-	Silicon
SiO_2	-	Silicon dioxide
SiF_4	-	Silicon tetrafluoride
SiF_6	-	Hexafluorosilicate
Ag_2O	-	Silver Oxide
NH_3	-	Ammonia
$Ag(NH_3)_2$	-	Di ammine silver(I)

LIST OF APPENDICES

APPENDIX	TITLE	PAGE
Appendix A	Real Picture of Un-cladding Process via Etching Method	177
Appendix B	Real Picture of Performance Analysis	178

CHAPTER 1

INTRODUCTION

1.1 Research Background

Optical fiber sensor is a device that exchanges the light rays into electronic signals and it has connected to a light source to allow the detection of modulated light. It measures the physical changes in the amount of light and translates it into a form of signal which is readable by the optical spectral analyzer. A multiple sensing application have been revolutionized by representing the fiber optic sensors. Possibility of preparing a variety of fiber sensing structures by glass and polymer optical fiber makes them an ideal candidate for fabrication of sensing device. Fiber optic sensors are generally classified as either intrinsic or extrinsic. In the intrinsic sensor, the physical properties of light inside the fiber are modulated by the physical detecting parameter whereas in an extrinsic sensor, light modulation occurs outside the fiber (Liaw, 2019). In the former, there is possibility to modulate one of the physical properties of the guided light such as wavelength, intensity, polarization and phase by the measurand. In the latter case, the fiber only acts as channel to transport the light signal to and from the sensor probe. However, out of these four properties of light, the intensity and wavelength modulated ones propose the widest range of optical fiber sensors (Du et al., 2019; Wang et al., 2018; Efendioglu, 2017). The special characteristics of being non-electrical, small in size, rugged and immune to electromagnetic interference boosts the use of optical fibers for sensing applications in the field of engineering, science and technology (Mowbray et al., 2019; Güemes, 2014). The physical and chemical properties such as temperature (Guo et al., 2019), liquid level (Díaz et al., 2019), radiation (Mikel et al., 2019), strain (Nascimento et al., 2019), refractive index (Gowri et al., 2019), vibration (Kuribayashi et al., 2019), concentration of liquid (Wang et al., 2019) and chemical analysis (Kaushik et al., 2019) can be detected by optical fiber sensors. Furthermore, low loss, low dispersion, ultra-wide bandwidth, high dynamic range, durability and upgradability are the other

reasons for shifting the attention from traditional electrical sensors to optical fiber sensors (Barrias et al., 2016). Compatibility to the multimode fiber technology and simplicity of construction are two main advantages of intensity and wavelength modulated sensors (Bag et al., 2020; Zhang et al., 2020).

1.2 Statement of the Problems

For developing the optical fiber sensor, the diameter of optical fiber must be reduced by removing the cladding part. Due to refraction of evanescent wave in the cladding and its absorption in surrounding media, the etched region of optical fiber becomes more sensitive (Korposh et al., 2019). For removing the cladding of optical fiber, several ways are existed. The current techniques for stripping the cladding can be divided into mechanical and chemical methods. Polishing the fiber is the most common mechanical technique to remove the cladding (Addanki et al., 2018). However, significant disadvantage of this method is that the fiber optic stripper can potentially damage the fiber core and it typically requires more expensive equipment. Furthermore, lasers and precision lenses on laser processing platforms with a moving mechanism are used for removing purpose, however, the precision lens on the laser processing platform tends to age, which may affect the accuracy of the moving platform and lead to cause experimental errors (Lin et al., 2019). Moreover, the problems such as an inability to correctly remove materials, and/or changes in the material properties may occur using the laser (Pospori et al., 2017). The chemical method like using of various solutions such as Hydrofluoric acid (HF) for glass optical fiber (GOF) and organic solvents for polymer optical fiber (POF) was employed by different researchers (Zaca-Morán et al., 2018; Razzaq et al., 2020; Subashini et al., 2018; Inglev et al., 2019). However, the etching process is difficult to control because a slight error can generate unexpected processing like damaging the core outer layer as a result affect the light propagating and sensing quality. Regardless of which method is employed, they all provide a lack of comprehensive post-processing quality control procedures.

It was discovered that the sensitivity of optical fiber sensors depends on the radius of the fiber, taper waist length, launch angle and surface roughness of the sensing area (Qazi et al., 2019; Rajamani et al., 2019; Qaziet al., 2019; Ma et al., 2019). Despite the fact that the light-scattering loss is increased by increasing the surface roughness, the sensors with rough surfaces exhibit higher sensitivity than those with smooth surfaces (Sequeira et al., 2019). The effects of core roughness after fully etching the cladding, on performance of conventional core-clad structure glass fiber sensors have previously been studied (Liu et al., 2002; Kim et al., 2010; Leal-Junior et al., 2018; Qazi et al., 2019), but the effects of cladding roughness associated with varying solvent concentration on sensitivity of partially unclad optical fiber probe have not been investigated extensively. Cladding thickness plays a crucial role on sensitivity of the sensor therefore, the removed cladding part in micrometer scale have been reported elsewhere. However, systematic and accurate control of cladding removal in nanometer have not been reported.

Currently, Ag coated optical fiber probe due to superior properties of Ag such as surface plasmon resonance (SPR), electron donor in dark and high reflectivity in the visual to near-infrared region has been attracted huge attention for measuring the refractive index changes (Fu et al., 2019; Lee et al., 2018; Shen et al., 2008). However, there is some backwards of using this material. Aging and exposing to atmosphere cases the oxygen deficit defects formed the silver oxide matrix on the sensing layer which consequences to shortening the life time and lowering the sensitivity of the fiber optic (Lee et al., 2018; Jiu et al., 2015). Moreover, high reflectivity leads to reflect the evanescent wave back completely to the core and prevent contacting with media.

Glass and polymer optical fiber as nonconductive substrates can be coated by chemical and physical vapor deposition (CVD and PVD), chemical electroless plating, sol gel and chemical bath deposition. However, continuous deposition type, high-temperature treatments and huge energy supply systems (Christopher et al., 2018; Ozcariz et al., 2019) which are required for PVD and CVD make them unsuitable for our purpose. In sol-gel method there is a little control over porosity of the gel which in turn affects the rate of solvent removal from the gel in order to form

the final powder and similar to the other methods, discontinuous coating also is not possible (Tang et al., 2017). Electroless plating is a promising technique for uniform metallic coating where discontinuous deposition would be possible however, deposition of different nanostructure configuration is not provided by this method. Moreover, it should be mentioned that in this study both glass and polymer fiber is employed to fabricate sensor due to extending their application and considering their pros and cons once using them in various devices and environment.

1.3 Objectives of the Study

Considering the research background and the problem statements mentioned before, the main objective of this study is to fabricate sensitive optical fiber probe to detect the refractive index variance of different liquids. The specific objectives are shown as follow:

- a) To fabricate partially unclad glass and polymer optical fiber sensors.
- b) To modify partially unclad optical fiber probe via ZnO/Ag bi-layer coating having ZnO nanoparticles and nanorods as an outer layer and investigate the influence of bi-layering on sensitivity.
- c) To evaluate and optimize the sensing parameters including shape of the zinc oxide nanostructure, length of the probe and propagating wavelength on sensor performance.

1.4 Scopes of the Research

For achieving the above stated objectives, following scopes of works have been presented:

- a) Preparing partially unclad glass and polymer multimode, step index optical fiber sensors for refractive index changes detection the following steps are performed:
 - i. Removing the part of cladding using dilute hydrofluoric acid in the range of 35-20 % with decreasing ratio of 5% for glass fiber and mixture of acetone/methanol in the range of (50/50), (40/60), (30/70) and (20/80) for polymer fiber. For both fibers the temperature varies from 15 to 30 °C by increasing ratio of 5 °C.
 - ii. Measuring the diameter of cladding using field emission scanning electron microscopy (FESEM) to observe the remain cladding thickness and its configuration. Atomic force microscopy (AFM) to obtain the cladding surface roughness. Dynamic monitoring system including solvents, broad band light source with a laser wavelength ranges from 360 to 2600 nm and power meter as a detector are employed. Higher (crude oil) and lower (saline) refractive index solutions with concentration of 0 to 100% and 0 to 20% are used respectively. The refractive index of the solution is measured by refractometer.
- b) For coating the fiber with ZnO/Ag bi-layer nanostructures and study their features following steps are carried out:
 - i. Electroless deposition technique is used for preparing the Ag nano-layers. The mixture of electroless, dip coating and low temperature hydrothermal method are employed for zinc oxide nanostructure deposition on top of the Ag layer.

- ii. Using field emission scanning electron microscopy (FESEM) the nanostructures size is measured and their shapes are observed. Energy dispersive X-ray spectroscopy (EDX) confirms the formation of deposited layer and examines the elemental distribution of the sample. X-Ray diffraction spectroscopy (XRD) estimates the degree of crystallinity and illustrates the structure of the deposited materials. Atomic force microscopy (AFM) reveals the morphology, size, roughness and surface topography of the fabricated probe. Contact angle (CA) is used to characterize the wettability of the probe surface. Zeta potential (ZP) is employed to determine the electrochemical surface properties and existence of charges on the surface. Photoluminescence (PL) spectroscopy determines the optical properties including the electronic bandgap, crystal defect energy level and changes the nanostructure band gap once exposing to different refractive index media. The UV-Vis/NIR transmission and absorption are employed for further optical characterization. Tensile test is carried out to measure the physical properties of the probe and its dependence to the applied stress. Refractometer measures the refractive index of the saline and crude oil solutions. Finally, the ImageJ program is applied to determine the dimension, size, and distribution of the ZnO nanostructure deposited on top.
-
- c) For fulfilling the third objective regarding to optimization of sensing parameters the following process is carried out.
 - i. Light sources of UV-Vis and IR (ranges from 360 nm to 2600 nm) are employed. The optical spectrum analyzer (OSA) is used as a light detector and multimode optical fibers having sensing length of 1 to 5 cm are applied. Saline and Crude oil solutions with different volume concentrations (ranges from 0 to 20% and 0 to 100%) are prepared as the measurand liquids.

1.5 Significance of Study

Nanosizing of materials is prerequisite for developing new electronic and optoelectronic devices. Especial miniature optical fiber sensors have sensitive thin films as a probe that can open new field in optical fiber sensor applications. Optical fibers act as signal carrier and thin films work as sensitive elements and transducer to get response and feedback from environments. The utilization of a highly sensitive, flexible, low cost, and small size intrinsic optical fiber sensor based on exterior cladding modifications for detecting the crude oil and saline concentration, permits operation at harsh environment with remote sensing operation capability, where bulk extrinsic sensors is not suitable to use. The magnitude of the salinity changes is a critical factor for determining the chemistry of natural waters and biological processes. The label-free refractive index sensor is promising device for detecting these changes. Therefore, an accurate monitoring of concentration changes in saline solution is prerequisite to control and minimize the negative effect of salt in water resources. Furthermore, efficient and accurate estimation of crude oil density changes is an essential factor in reservoir engineering. Determining the refractive index gradient as a representative of these changes by optical fiber sensor offers a novel approach in oil production optimization.

A novel ZnO/Ag bi-layer coated intensity and wavelength modulated optical fiber sensors having variety of ZnO shapes based on refractive index changes using IR and UV-Vis light sources are proposed. It is believed that this is the first work that the economic electroless technique as a promising chemical method is used for bi-layer deposition of materials on multimode optical fiber. Moreover, controlling the ZnO nanostructure shape which has direct effect on sensing mechanism can be controlled by chemical techniques and has not been extensively done. The possibility of tuning the optical response of coated nanomaterials by modifying their cladding part, synthesize techniques, length of the sensing area, nanostructure configuration and applying different light source has become one of the most challenging aspects of recent fiber optic sensor research and have been successfully fulfilled in this thesis.

For controlling the assembly process and maintaining the quality of final products in manufacturing development where remote sensing is demanded, our organized fabricated micro scale sensor with low disturbance and without any explosion risks can contribute more effectively than the other types of sensors. The proposed fabrication technique would be easy and economic. Large-scale and socio-economic instrumentation is provided. The fundamental phenomena and details of sensing mechanism would be fully understood. The device fabricated by this research can be used in a wide range of industries and the data created will be published in high impact factor journal and presented in workshops, conferences and seminars. This methodology can be used to train the PhD and masters research scholar. High quality home fabricated optical fiber sensors can support the demands in optoelectronic industries. Measuring the small changes in refractive index would be possible by a set of characterization that is proposed. A right fiber optic sensor configuration for refractive index monitoring will be offered. These methodologies are not just limited to the deposited silver and zinc oxide nanostructures and it can be extended to other materials based on application needed. Other nanostructure materials like gold, nickel, copper and other also can be used as sensing part.

1.6 Organization of Thesis

This thesis structurally is divided into five chapters giving a complete fabrication, characterization and performance on partially unclad optical fiber sensors coated with bi layer ZnO/Ag for developing optical fiber sensors to monitor refractive index (concentration) of saline and crude oil solutions. The current chapter presents a short introduction on fiber optics field that consist of the motivation and the objectives of this research.

Chapter 2 provides more information of an available literature review. This chapter consists of the theory of sensing mechanism and classification of optical fiber probe considering different aspects. Moreover, the feature and potential of ZnO and Ag as sensitive coated materials are extensively discussed. Varieties of deposition techniques are listed and among them electroless method is explained.

Chapter 3 includes a description of the fabrication of glass and polymer partially unclad optical fiber sensors based on solvent concentration and temperature. Moreover, fabricating of polymer and glass probe using deposition of bi-layer ZnO/Ag having different configuration of ZnO on partially unclad optical fiber via mixture of three techniques of electroless, dip coating and low temperature hydrothermal method are explained. Finally, background information of major experimental tools or techniques for collecting data is explained.

In chapter 4 the fabricated partially unclad optical fiber is characterized to view the morphology, structure and its performance. The role of probe length and etching solution concentration discussed in detail and the results are presented. Then, the optical features of ZnO/Ag nanostructures are investigated. The performance of ZnO/Ag bi-layer coated on polymer and glass fiber having variety of top-layer configurations is studied and presented. The sensitivity comparison for all fabricated probe is carried out and listed. Physical characteristic of the polymer and glass fiber sensor fabricated with optimum parameters is studied.

Chapter 5 gives a summary and review of the results and analysis of this study. It additionally includes limitation of this research and suggestions for further research work. Attached in the appendix contain published papers during this study.

REFERENCES

- Addanki, S., Amiri, I.S. and Yupapin, P. (2018) Review of optical fibers-introduction and applications in fiber lasers, *Results in Physics*, 10, pp.743-750.
- Ahmad, M. and Hensch, L.L. (2005) Effect of taper geometries and launch angle on evanescent wave penetration depth in optical fibers. *Biosensors and Bioelectronics*, 20(7), pp.1312-1319.
- Allwood, G., Wild, G. and Hinckley, S. (2016) Optical fiber sensors in physical intrusion detection systems: A review. *IEEE Sensors Journal*, 16(14), pp.5497-5509.
- Alomair, O., Jumaa, M., Alkorieh, A. and Hamed, M. (2016) Heavy oil viscosity and density prediction at normal and elevated temperatures. *Journal of Petroleum Exploration and Production Technology*, 6(2), pp.253-263.
- Al-Qazwini, Y., Noor, A.S.M., Al-Qazwini, Z., Yaacob, M.H., Harun, S.W. and Mahdi, M.A. (2016) Refractive index sensor based on SPR in symmetrically etched plastic optical fibers. *Sensors and Actuators A: Physical*, 246, pp.163-169.
- Amiri, I.S., Alwi, S.A.K., Raya, S.A., Zainuddin, N.A.A.M., Rohizat, N.S., Rajan, M.M. and Zakaria, R. (2019) Graphene oxide effect on improvement of silver surface plasmon resonance D-shaped optical fiber sensor. *Journal of Optical Communications*, pp.1-8.
- Ascorbe, J., Corres, J.M., Del Villar, I. and Matias, I.R. (2018) Fabrication of long period gratings by periodically removing the coating of cladding-etched single mode optical fiber towards optical fiber sensor development. *Sensors*, 18(6), p.1866.
- Ascorbe, J., Corres, J.M., Matias, I.R. and Arregui, F.J. (2016) High sensitivity humidity sensor based on cladding-etched optical fiber and lossy mode resonances. *Sensors and Actuators B: Chemical*, 233, pp.7-16.
- Azad, S., Sadeghi, E., Parvizi, R., Mazaheri, A. and Yousefi, M. (2017) Sensitivity optimization of ZnO clad-modified optical fiber humidity sensor by means of tuning the optical fiber waist diameter. *Optics & Laser Technology*, 90, pp.96-101.

- Bag, S.K., Wan, M., Sinha, R.K. and Varshney, S.K. (2020) Design and Characterization of Surface Relief Grating on Etched Multimode Optical Fiber for Refractive Index Sensing. *Sensors and Actuators A: Physical*, p.111836.
- Ballato, J. and Dragic, P. (2014) Materials development for next generation optical fiber. *Materials*, 7(6), pp.4411-4430.
- Bao, W., Qiao, X., Yin, X., Rong, Q., Wang, R. and Yang, H. (2017) Optical fiber micro-displacement sensor using a refractive index modulation window-assisted reflection fiber taper. *Optics Communications*, 405, pp.276-280.
- Bao, Y., Huang, Y., Hoehler, M.S. and Chen, G., 2019. Review of fiber optic sensors for structural fire engineering. *Sensors*, 19(4), p.877.
- Baptista, A., Silva, F., Porteiro, J., Míguez, J. and Pinto, G. (2018) Sputtering physical vapour deposition (PVD) coatings: A critical review on process improvement and market trend demands. *Coatings*, 8(11), p.402.
- Barrias, A., Casas, J.R. and Villalba, S. (2016) A review of distributed optical fiber sensors for civil engineering applications. *Sensors*, 16(5), p.748.
- Bhardwaj, V. and Singh, V.K. (2016) Fabrication and characterization of cascaded tapered Mach-Zehnder interferometer for refractive index sensing. *Sensors and Actuators A: Physical*, 244, pp.30-34.
- Biswas, R. and Pradhan, M. (2020) A comparative analysis of all fiber optic sensors for detection of adulteration in fossil fuels. *Optical and Quantum Electronics*, 52(2), p.62.
- Bosch-Navarro, C., Rourke, J.P. and Wilson, N.R. (2016) Controlled electrochemical and electroless deposition of noble metal nanoparticles on graphene. *RSC advances*, 6(77), pp.73790-73796.
- Bremer, K., Alwis, L.S.M., Zheng, Y. and Roth, B.W. (2020). Towards Mode-Multiplexed Fiber Sensors: An Investigation on the Spectral Response of Etched Graded Index OM4 Multi-Mode Fiber with Bragg grating for Refractive Index and Temperature Measurement. *Applied Sciences*, 10(1), p.337.
- Bunge, C.A., Beckers, M. and Gries, T. eds. (2016) Polymer Optical Fibres: Fibre Types, Materials, Fabrication, Characterisation and Applications. *Woodhead Publishing*.

- Cao, J., Galbraith, E.K., Sun, T. and Grattan, K.T.V (2011). Comparison of surface plasmon resonance and localized surface plasmon resonance-based optical fibre sensors. *In Journal of Physics: Conference Series*, 307(1), p. 012050.
- Cennamo, N., Pesavento, M., Marchetti, S. and Zeni, L. (2020) Molecularly Imprinted Polymers and Optical Fiber Sensors for Security Applications. *In Advanced Materials for Defense* (pp. 17-24). Springer, Cham.
- Chai, B.H., Zheng, J.M., Zhao, Q. and Pollack, G.H. (2008) Spectroscopic studies of solutes in aqueous solution. *The Journal of Physical Chemistry A*, 112(11), pp.2242-2247.
- Chamkalani, A., 2012. Correlations between SARA fractions, density, and RI to investigate the stability of asphaltene. *ISRN Analytical Chemistry*, 2012.
- Chen, C.H., Wu, W.T. and Wang, J.N. (2017) All-fiber microfluidic multimode Mach–Zehnder interferometers as high sensitivity refractive index sensors. *Microsystem Technologies*, 23(2), pp.429-440.
- Chen, H. and Ruckenstein, E. (2015) Hydrated ions: from individual ions to ion pairs to ion clusters. *The Journal of Physical Chemistry B*, 119(39), pp.12671-12676.
- Chen, J., Bamiedakis, N., Vasil'ev, P.P., Edwards, T.J., Brown, C.T., Penty, R.V. and White, I.H. (2016) High-bandwidth and large coupling tolerance graded-index multimode polymer waveguides for on-board high-speed optical interconnects. *Journal of Lightwave Technology*, 34(12), pp.2934-2940.
- Cho, C.Y., Kim, N.Y., Kang, J.W., Leem, Y.C., Hong, S.H., Lim, W., Kim, S.T. and Park, S.J. (2013) Improved light extraction efficiency in blue light-emitting diodes by SiO₂-coated ZnO nanorod arrays. *Applied Physics Express*, 6(4), p.042102.
- Christopher, C., Subrahmanyam, A. and Sai, V.V.R. (2018) Gold sputtered U-bent plastic optical fiber probes as SPR-and LSPR-based compact plasmonic sensors. *Plasmonics*, 13(2), pp.493-502.
- Chyad, R.M., Jafri, M.Z.M. and ulazizi Ibrahim, K. (2015) Fabrication nano fiber optic by chemical etching for sensing application. *Engineering and Technology Journal*, 33(6 Part (B) Scientific), pp.994-1002.

- Cui, Z., Gong, J., Wang, C., Che, N., Zhao, Y., Chai, Q., Qi, H., Lewis, E., Ren, J., Zhang, J. and Yang, J. (2019) Observing the viscous relaxation process of silica optical fiber at~ 1000 C using regenerated fiber bragg grating. *Sensors*, 19(10), p.2293.
- Dash, J.G. (1999) History of the search for continuous melting. *Reviews of Modern Physics*, 71(5), p.1737.
- Dastmalchi, B., Tassin, P., Koschny, T. and Soukoulis, C.M. (2016) A new perspective on plasmonics: confinement and propagation length of surface plasmons for different materials and geometries. *Advanced Optical Materials*, 4(1), pp.177-184.
- de Andrés, A.I., O’Keeffe, S., Chen, L. and Esteban, Ó. (2017) Highly sensitive extrinsic X-ray polymer optical fiber sensors based on fiber tip modification. *IEEE Sensors Journal*, 17(16), pp.5112-5117.
- Di Sante, R. (2015) Fibre optic sensors for structural health monitoring of aircraft composite structures: Recent advances and applications. *Sensors*, 15(8), pp.18666-18713.
- Díaz, C.A., Leal-Junior, A., Marques, C., Frizera, A., Pontes, M.J., Antunes, P.F., André, P.S. and Ribeiro, M.R. (2019) Optical fiber sensing for sub-millimeter liquid-level monitoring: a review. *IEEE Sensors Journal*, 19(17), pp.7179-7191.
- Du, Y., Han, Q., Hu, H., Sang, M., Zhao, X., Song, X., Wang, H. and Liu, T. (2019) High-sensitivity refractive index and temperature sensor based on cascading FBGs and droplet-like fiber interferometer. *Sensors and Actuators A: Physical*, 299, p.111631.
- Duarte, D.P., Nogueira, R.N. and Bilro, L.B. (2020) A low-cost liquid refractive index sensor based on plastic optical fibre and CCD array. *Measurement Science and Technology*, 31(4), p.047001.
- Dubey, P.K. and Shukla, V. (2014) Dispersion in Optical Fiber Communication. *International Journal of Science & Research (IJSR), India*, 3(10), pp.236-239.
- Efendioglu, H.S. (2017) A review of fiber-optic modal modulated sensors: Specklegram and modal power distribution sensing. *IEEE Sensors Journal*, 17(7), pp.2055-2064.

- Essiambre, R.J., Kramer, G., Winzer, P.J., Foschini, G.J. and Goebel, B. (2010) Capacity limits of optical fiber networks. *Journal of Lightwave Technology*, 28(4), pp.662-701.
- Fabijanić, I., Janicki, V., Ferré-Borrull, J., Bubaš, M., Blažek Bregović, V., Marsal, L.F. and Sancho-Parramon, J. (2019) Plasmonic Nanoparticles and Island Films for Solar Energy Harvesting: A Comparative Study of Cu, Al, Ag and Au Performance. *Coatings*, 9(6), p.382.
- Flaes, D.E.B., Stopka, J., Turtaev, S., De Boer, J.F., Tyc, T. and Čižmár, T. (2018) Robustness of light-transport processes to bending deformations in graded-index multimode waveguides. *Physical review letters*, 120(23), p.233901.
- Fotovvati, B., Namdari, N. and Dehghanhadikolaei, A. (2019) On coating techniques for surface protection: a review. *Journal of Manufacturing and Materials Processing*, 3(1), p.28.
- Fu, H., Jiang, Y., Ding, J., Zhang, J., Zhang, M., Zhu, Y. and Li, H. (2018) Zinc oxide nanoparticle incorporated graphene oxide as sensing coating for interferometric optical microfiber for ammonia gas detection. *Sensors and Actuators B: Chemical*, 254, pp.239-247.
- Fu, H., Zhang, M., Ding, J., Wu, J., Zhu, Y., Li, H., Wang, Q. and Yang, C. (2019) A high sensitivity D-type surface plasmon resonance optical fiber refractive index sensor with graphene coated silver nano-columns. *Optical Fiber Technology*, 48, pp.34-39.
- Gangopadhyay, T.K., Halder, A., Das, S., Paul, M.C., Pal, M., Salza, M. and Gagliardi, G. (2011) Fabrication of tapered single mode fiber by chemical etching and used as a chemical sensor based on evanescent field absorption. *Tenth International Conference on Fiber Optics and Photonics*, 8173, p. 817321.
- Ghetia, S., Gajjar, R. and Trivedi, P. (2013) Classification of fiber optical sensors. *International Journal of Electronics Communication and Computer Technology*, 3, pp.442-445.
- Gobi, G., Sastikumar, D., Balaji Ganesh, A. and Radhakrishnan, T. (2009) Fiber-optic sensor to estimate surface roughness of corroded metals. *Optica Applicata*, pp.5-10.

- Gomes, N.J., Morant, M., Alphones, A., Cabon, B., Mitchell, J.E., Lethien, C., Csörnyei, M., Stöhr, A. and Iezekiel, S. (2009) Radio-over-fiber transport for the support of wireless broadband services. *Journal of Optical Networking*, 8(2), pp.156-178.
- Gowri, A., Rajamani, A.S., Ramakrishna, B. and Sai, V.V.R. (2019) U-bent plastic optical fiber probes as refractive index based fat sensor for milk quality monitoring. *Optical Fiber Technology*, 47, pp.15-20.
- Güemes, A. (2014) Fiber Optics Strain Sensors. *NATO-STO Lecture Series (STO-EN-AVT-220)*, 16.
- Guo, J., Zhou, B., Yang, C., Dai, Q. and Kong, L. (2019) Stretchable and Temperature-Sensitive Polymer Optical Fibers for Wearable Health Monitoring. *Advanced Functional Materials*, 29(33), p.1902898.
- Gupta, B.D., Shrivastav, A.M. and Usha, S.P. (2016) Surface plasmon resonance-based fiber optic sensors utilizing molecular imprinting. *Sensors*, 16(9), p.1381.
- Hammond, J.L., Bhalla, N., Rafiee, S.D. and Estrela, P. (2014) Localized surface plasmon resonance as a biosensing platform for developing countries. *Biosensors*, 4(2), pp.172-188.
- Hassan, A., Jin, Y., Irfan, M. and Jiang, Y. (2018) Acceptor-modulated optical enhancements and band-gap narrowing in ZnO thin films. *AIP Advances*, 8(3), p.035212.
- Hassan, H.U., Bang, O. and Janting, J. (2019) Polymer optical fiber tip mass production etch mechanism to achieve CPC shape for improved biosensor performance. *Sensors*, 19(2), p.285.
- Herve, P. and Vandamme, L.K.J. (1994) General relation between refractive index and energy gap in semiconductors. *Infrared physics & technology*, 35(4), pp.609-615.
- Herve, P.J.L. and Vandamme, L.K.J. (1995) Empirical temperature dependence of the refractive index of semiconductors. *Journal of Applied Physics*, 77(10), pp.5476-5477.
- Hisham, H.K. (2018) Optical fiber sensing technology: Basics, classifications and applications. *American Journal of Remote Sensing*, 6(1), pp.1-5.

- Hribar, B., Southall, N.T., Vlachy, V. and Dill, K.A. (2002) How ions affect the structure of water. *Journal of the American Chemical Society*, 124(41), pp.12302-12311.
- Huang, L., Yao, T., Leng, J., Guo, S., Tao, R. and Zhou, P. (2017) Mode instability dynamics in high-power low-numerical-aperture step-index fiber amplifier. *Applied optics*, 56(19), pp.5412-5417.
- Huang, X., Li, X., Yang, J., Tao, C., Guo, X., Bao, H., Yin, Y., Chen, H. and Zhu, Y. (2017) An in-line Mach-Zehnder interferometer using thin-core fiber for ammonia gas sensing with high sensitivity. *Scientific reports*, 7, p.44994.
- Huang, Y., Wang, T., Deng, C., Zhang, X., Pang, F., Bai, X., Dong, W., Wang, L. and Chen, Z. (2017) A highly sensitive intensity-modulated optical fiber magnetic field sensor based on the magnetic fluid and multimode interference. *Journal of Sensors*, 2017.
- Idris, N.F., Yahya, N.A.M., Yaacob, M.H., Idris, A.H., Harun, S.W. and Saidin, N. (2019) Optical fiber coated Zinc Oxide (ZnO) nanorods decorated with Palladium (Pd) for hydrogen sensing. *Optical Materials*, 96, p.109291.
- Indolia, R. (2017) Relationship of refractive index with optical energy gap and average energy gap for II-VI and III-V group of semiconductors. *Int. J. Pure Appl. Phys*, 13(2), pp.185-191.
- Inglev, R., Woyessa, G., Bang, O. and Janting, J. (2019) Polymer Optical Fiber Modification By Etching Using Hansen Solubility Parameters—A Case Study of TOPAS, Zeonex, and PMMA. *Journal of Lightwave Technology*, 37(18), pp.4776-4783.
- Irawati, N., Rahman, H.A., Ahmad, H. and Harun, S.W. (2017) A PMMA microfiber loop resonator based humidity sensor with ZnO nanorods coating. *Measurement*, 99, pp.128-133.
- Irigoyen, M., Sánchez-Martin, J.A., Bernabeu, E. and Zamora, A. (2017) Tapered optical fiber sensor for chemical pollutants detection in seawater. *Measurement Science and Technology*, 28(4), p.045802.
- Jagtap, S., Rane, S., Arbuji, S., Rane, S. and Gosavi, S. (2018) Optical fiber based humidity sensor using Ag decorated ZnO nanorods. *Microelectronic Engineering*, 187, pp.1-5.

- Jali, M.H., Rahim, H.R.A., Yusof, H.H.M., Johari, M.A.M., Thokchom, S., Harun, S.W. and Yasin, M. (2019) Optimization of sensing performance factor (γ) based on microfiber-coupled ZnO nanorods humidity scheme. *Optical Fiber Technology*, 52, p.101983.
- Jin, C., Li, J., Han, S., Wang, J., Yao, Q. and Sun, Q. (2015) Silver mirror reaction as an approach to construct a durable, robust superhydrophobic surface of bamboo timber with high conductivity. *Journal of Alloys and Compounds*, 635, pp.300-306.
- Jiu, J., Wang, J., Sugahara, T., Nagao, S., Nogi, M., Koga, H., Suganuma, K., Hara, M., Nakazawa, E. and Uchida, H. (2015) The effect of light and humidity on the stability of silver nanowire transparent electrodes. *RSC Advances*, 5(35), pp.27657-27664.
- Joe, H.E., Yun, H., Jo, S.H., Jun, M.B. and Min, B.K. (2018) A review on optical fiber sensors for environmental monitoring. *International journal of precision engineering and manufacturing-green technology*, 5(1), pp.173-191.
- Kant, R., Tabassum, R. and Gupta, B.D. (2016) Fiber optic SPR-based uric acid biosensor using uricase entrapped polyacrylamide gel. *IEEE Photonics Technology Letters*, 28(19), pp.2050-2053.
- Kaushik, S., Tiwari, U.K., Deep, A. and Sinha, R.K. (2019) Two-dimensional transition metal dichalcogenides assisted biofunctionalized optical fiber SPR biosensor for efficient and rapid detection of bovine serum albumin. *Scientific reports*, 9(1), pp.1-11.
- Kavinkumar, T. and Manivannan, S. (2016) Uniform decoration of silver nanoparticle on exfoliated graphene oxide sheets and its ammonia gas detection. *Ceramics International*, 42(1), pp.1769-1776.
- Kbashi, H.J. (2012) Fabrication of submicron-diameter and taper fibers using chemical etching. *Journal of Materials Science & Technology*, 28(4), pp.308-312.
- Kim, H.J., Kwon, O.J. and Han, Y.G. (2010) Effect of surface roughness variation on the transmission characteristics of D-shaped fibers with ambient index change. *Journal of the Korean Physical Society*, 56(42), pp.1355-1358.

- Ko, S., Lee, J., Koo, J., Joo, B.S., Gu, M. and Lee, J.H. (2016) Chemical wet etching of an optical fiber using a hydrogen fluoride-free solution for a saturable absorber based on the evanescent field interaction. *Journal of Lightwave Technology*, 34(16), pp.3776-3784.
- Ko, Y.C., Melani, L., Park, N.Y. and Kim, H.J. (2019) Surface characterization of paper and paperboard using a stylus contact method. *Nordic Pulp & Paper Research Journal*, 10(15), pp 1-10.
- Korposh, S., James, S.W., Lee, S.W. and Tatam, R.P. (2019) Tapered optical fibre sensors: Current trends and future perspectives. *Sensors*, 19(10), p.2294.
- Korposh, S., Kodaira, S., Selyanchyn, R., Ledezma, F.H., James, S.W. and Lee, S.W. (2018) Porphyrin-nanoassembled fiber-optic gas sensor fabrication: Optimization of parameters for sensitive ammonia gas detection. *Optics & Laser Technology*, 101, pp.1-10.
- Kumar, J., Prakash, O., Mahakud, R., Agrawal, S.K., Dixit, S.K., Nakhe, S.V. and Canning, J. (2017) Wavelength independent chemical sensing using etched thermally regenerated FBG. *Sensors and Actuators B: Chemical*, 244, pp.54-60.
- Kumar, M., Kumar, A. and Tripathi, S.M. (2014) A comparison of temperature sensing characteristics of SMS structures using step and graded index multimode fibers. *Optics Communications*, 312, pp.222-226.
- Kumar, V. and Singh, J.K. (2010) Model for calculating the refractive index of different materials. *Indian journal of pure and applied physics*, 48, pp.571-574.
- Kuribayashi, K., Nagase, R. and Wada, S. (2019) October. Study of Vibration Sensing Technique Using Fabry-Pérot Interferometer with Optical Fibers. *In IECON 2019-45th Annual Conference of the IEEE Industrial Electronics Society* (Vol. 1, pp. 7143-7147). IEEE.
- Lah, C.N.H.C., Jamaludin, N., Rokhani, F.Z., Rashid, S.A. and Noor, A.S.M. (2019) Lard detection using a tapered optical fiber sensor integrated with gold-graphene quantum dots. *Sensing and Bio-Sensing Research*, 26, p.100306.
- Leal-Junior, A.G., Frizera, A. and Pontes, M.J. (2018) Sensitive zone parameters and curvature radius evaluation for polymer optical fiber curvature sensors. *Optics & Laser Technology*, 100, pp.272-281.

- Lee, M.K., Kim, T.G., Kim, W. and Sung, Y.M. (2008) Surface plasmon resonance (SPR) electron and energy transfer in noble metal– zinc oxide composite nanocrystals. *The Journal of Physical Chemistry C*, 112(27), pp.10079-10082.
- Lee, S.H., Jo, J.S., Park, J.H., Lee, S.W. and Jang, J.W. (2018) A hot-electron-triggered catalytic oxidation reaction of plasmonic silver nanoparticles evidenced by surface potential mapping. *Journal of Materials Chemistry A*, 6(42), pp.20939-20946.
- Li, C., Feng, C.Q., Zhu, D.Y., Liu, S.B. and An, Q. (2018) An optical fiber-based flexible readout system for micro-pattern gas detectors. *Journal of Instrumentation*, 13(04), p.P04013.
- Li, M. and Li, J.C. (2006) Size effects on the band-gap of semiconductor compounds. *Materials Letters*, 60(20), pp.2526-2529.
- Li, X., Shao, Y., Yu, Y., Zhang, Y. and Wei, S. (2016) A highly sensitive fiber-optic Fabry–Perot interferometer based on internal reflection mirrors for refractive index measurement. *Sensors*, 16(6), p.794.
- Liaw, S.K. An Overview the Methodologies and Applications of Fiber Optic Sensing. *In Fiber Optic Sensing-Principle, Measurement and Applications: Wiley*, 1-14; 2019.
- Lin, J.H., Lin, C.H., Tai, P.T. and Yen, W.C. *National Chung Shan Institute of Science, High power optical fiber laser combiner*. U.S. Patent 10, 396, 524. 2019.
- Lin, K.F., Cheng, H.M., Hsu, H.C., Lin, L.J. and Hsieh, W.F. (2005) Band gap variation of size-controlled ZnO quantum dots synthesized by sol–gel method. *Chemical Physics Letters*, 409(4-6), pp.208-211.
- Lindgren, E. A. Screen Room Air Inlet and Wave Guard. V.S. Patent 2, 925,457. 1960.
- Liu, J., Yamazaki, K., Zhou, Y. and Matsumiya, S. (2002) A reflective fiber optic sensor for surface roughness in-process measurement. *J. Manuf. Sci. Eng.*, 124(3), pp.515-522.
- Liu, W., Wu, X., Zhang, G., Li, S., Zuo, C., Fang, S. and Yu, B. (2020) Refractive index and temperature sensor based on Mach-Zehnder interferometer with thin fibers. *Optical Fiber Technology*, 54, p.102101.

- Liu, Y., Li, P., Zhang, N., Zhang, X., Chen, S., Liu, Z., Guang, J. and Peng, W. (2019) Fiber-optic evanescent field humidity sensor based on a micro-capillary coated with graphene oxide. *Optical Materials Express*, 9(11), pp.4418-4428.
- Liu, Z., Zhang, Z.F., Tam, H.Y. and Tao, X. (2019) Multifunctional smart optical fibers: Materials, fabrication, and sensing applications. *In Photonics*, 6(2), p.48.
- Lobnik, A., Turel, M. and Urek, Š. (2012) Optical chemical sensors: Design and applications. *Advances in Chemical Sensors*, pp.3-28.
- Ma, G.M., Zhou, H.Y., Zhang, M., Li, C.R., Yin, Y. and Wu, Y.Y. (2019) A high sensitivity optical fiber sensor for GIS partial discharge detection. *IEEE Sensors Journal*, 19(20), pp.9235-9243.
- Mallory, G.O. and Hajdu, J.B. eds. *Electroless plating: fundamentals and applications*. Cambridge University Press: AESF. 1990.
- Malshe, A.P., Park, B.S., Brown, W.D. and Naseem, H.A. (1999) A review of techniques for polishing and planarizing chemically vapor-deposited (CVD) diamond films and substrates. *Diamond and Related Materials*, 8(7), pp.1198-1213.
- Marczak, R., Werner, F., Gniewitz, J.F., Hirsch, A., Guldi, D.M. and Peukert, W. (2009) Communication via electron and energy transfer between zinc oxide nanoparticles and organic adsorbates. *The Journal of Physical Chemistry C*, 113(11), pp.4669-4678.
- Mayer, K.M. and Hafner, J.H. (2011) Localized surface plasmon resonance sensors. *Chemical reviews*, 111(6), pp.3828-3857.
- McPeak, K.M., Jayanti, S.V., Kress, S.J., Meyer, S., Iotti, S., Rossinelli, A. and Norris, D.J. (2015) Plasmonic films can easily be better: rules and recipes. *ACS photonics*, 2(3), pp.326-333.
- Menon, V.P. and Martin, C.R. (1995) Fabrication and evaluation of nanoelectrode ensembles. *Analytical Chemistry*, 67(13), pp.1920-1928.
- Mikel, B., Jelínek, M., Rerucha, S., Hrabina, J. and Cip, O. (2019) October. Ionizing radiation measurement using optical fibers. In Seventh European Workshop on Optical Fibre Sensors (Vol. 11199, p. 111993M). *International Society for Optics and Photonics*.

- Minnes, R., Brider, T., Goryachev, A., Grushchenko, A., Tor, R., Nevo, A., Lifshitz, D., Katzir, A. and Raichlin, Y. (2019) Fiber-optic evanescent wave spectroscopy (FEWS) of crystals from a urine sample as a tool for evaluating the chemical composition of kidney stones. *Analytical Methods*, 11(18), pp.2404-2409.
- Moss, T.S. (1985) Relations between the refractive index and energy gap of semiconductors. *physica status solidi (b)*, 131(2), pp.415-427.
- Mowbray, S.E. and Amiri, A.M. (2019) A brief overview of medical fiber optic biosensors and techniques in the modification for enhanced sensing ability. *Diagnostics*, 9(1), p.23.
- Mozumder, M.S., Mourad, A.H.I., Pervez, H. and Surkatti, R. (2019) Recent developments in multifunctional coatings for solar panel applications: A review. *Solar Energy Materials and Solar Cells*, 189, pp.75-102.
- Nadarajah, K., Yern Chee, C. and Tan, C.Y. (2013) Influence of annealing on properties of spray deposited ZnO thin films. *Journal of Nanomaterials*, 2013, pp.1-8.
- Nascimento, M., Novais, S., Ding, M.S., Ferreira, M.S., Koch, S., Passerini, S. and Pinto, J.L. (2019) Internal strain and temperature discrimination with optical fiber hybrid sensors in Li-ion batteries. *Journal of Power Sources*, 410, pp.1-9.
- Ng, W.L., Rifat, A.A., Wong, W.R., Mahdiraji, G.A. and Adikan, F.M. (2018) A novel diamond ring fiber-based surface plasmon resonance sensor. *Plasmonics*, 13(4), pp.1165-1170.
- Ning, Y.N., Grattan, K.T.V., Wang, W.M. and Palmer, A.W. (1991) A systematic classification and identification of optical fibre sensors. *Sensors and Actuators A: Physical*, 29(1), pp.21-36.
- Ojha, N.S., Kumar, A. and Kumar, N. (2020) Post-fabrication refractive index sensitivity enhancement technique for single-fiber Mach-Zehnder interferometer. *Optical Fiber Technology*, 54, p.102118.
- Ozcariz, A., Dominik, M., Smietana, M., Zamarreño, C.R., Del Villar, I. and Arregui, F.J. (2019) Lossy mode resonance optical sensors based on indium-gallium-zinc oxide thin film. *Sensors and Actuators A: Physical*, 290, pp.20-27.

- Pahurkar, V.G., Tamgadge, Y.S., Gambhire, A.B. and Muley, G.G. (2015) Evanescent wave absorption based polyaniline cladding modified fiber optic intrinsic biosensor for glucose sensing application. *Measurement*, 61, pp.9-15.
- Palstra, T.T.M., Batlogg, B., Van Dover, R.B., Schneemeyer, L.F. and Waszczak, J.V. (1990) Dissipative flux motion in high-temperature superconductors. *Physical Review B*, 41(10), p.6621.
- Pathak, A.K., Chaudhary, D.K. and Singh, V.K. (2018) Broad range and highly sensitive optical pH sensor based on Hierarchical ZnO microflowers over tapered silica fiber. *Sensors and Actuators A: Physical*, 280, pp.399-405.
- Pawar, D. and Kale, S.N. (2019) A review on nanomaterial-modified optical fiber sensors for gases, vapors and ions. *Microchimica Acta*, 186(4), p.253.
- Pawar, D., Kitture, R. and Kale, S.N. (2017) ZnO coated Fabry-Perot interferometric optical fiber for detection of gasoline blend vapors: Refractive index and fringe visibility manipulation studies. *Optics & Laser Technology*, 89, pp.46-53.
- Pitarke, J.M., Silkin, V.M., Chulkov, E.V. and Echenique, P.M. (2006). Theory of surface plasmons and surface-plasmon polaritons. *Reports on progress in physics*, 70(1), p.1.
- Pospori, A., Marques, C.A., Bang, O., Webb, D.J. and André, P. (2017) Polymer optical fiber Bragg grating inscription with a single UV laser pulse. *Optics express*, 25(8), pp.9028-9038.
- Prasood, U.S., Mishra, S.K. and Gupta, B.D. (2014) December. Surface Plasmon Resonance Based Fiber Optic Chlorine Gas Sensor Utilizing Ag/Zno Thin Film. In International Conference on Fibre Optics and Photonics, *Optical Society of America*, (pp. M4A-52).
- Preda, N., Evangelidis, A., Enculescu, M., Florica, C. and Enculescu, I. (2015) Zinc oxide electroless deposition on electrospun PMMA fiber mats. *Materials Letters*, 138, pp.238-242.
- Preda, N., Evangelidis, A., Enculescu, M., Florica, C. and Enculescu, I. (2015) Zinc oxide electroless deposition on electrospun PMMA fiber mats. *Materials Letters*, 138, pp.238-242.

- Presti, D.L., Massaroni, C., Piemonte, V., Saccomandi, P., D'Amato, R., Caponero, M.A. and Schena, E. (2019) Agar-coated fiber Bragg grating sensor for relative humidity measurements: Influence of coating thickness and polymer concentration. *IEEE Sensors Journal*, 19(9), pp.3335-3342.
- Pulido, C. and Esteban, Ó. (2010) Improved fluorescence signal with tapered polymer optical fibers under side-illumination. *Sensors and Actuators B: Chemical*, 146(1), pp.190-194.
- Qazi, H.H., Memon, S.F., Ali, M.M., Irshad, M.S., Ehsan, S.A., Salim, M.R.B., Mohammad, A.B.B., Zulkifli, M.Z. and Idrees, M. (2019) Surface roughness and the sensitivity of D-shaped optical fibre sensors. *Journal of Modern Optics*, 66(11), pp.1244-1251.
- Qi, W.H. (2005) Size effect on melting temperature of nanosolids. *Physica B: Condensed Matter*, 368(1-4), pp.46-50.
- Rahman, M.S., Anower, M.S., Rahman, M.K., Hasan, M.R., Hossain, M.B. and Haque, M.I. (2017) Modeling of a highly sensitive MoS₂-Graphene hybrid based fiber optic SPR biosensor for sensing DNA hybridization. *Optik*, 140, pp.989-997.
- Raj, D.R., Prasanth, S., Vineeshkumar, T.V. and Sudarsanakumar, C. (2015) Ammonia sensing properties of tapered plastic optical fiber coated with silver nanoparticles/PVP/PVA hybrid. *Optics Communications*, 340, pp.86-92.
- Raj, D.R., Prasanth, S., Vineeshkumar, T.V. and Sudarsanakumar, C. (2016) Surface plasmon resonance based fiber optic dopamine sensor using green synthesized silver nanoparticles. *Sensors and Actuators B: Chemical*, 224, pp.600-606.
- Rajamani, A.S., Divagar, M. and Sai, V.V.R. (2019) Plastic fiber optic sensor for continuous liquid level monitoring. *Sensors and Actuators A: Physical*, 296, pp.192-199.
- Rajan, G., Shouha, P., Ellakwa, A., Bhowmik, K., Xi, J. and Prusty, G. (2016) Evaluation of the physical properties of dental resin composites using optical fiber sensing technology. *Dental Materials*, 32(9), pp.1113-1123.
- Rashid, A.R.A., Nasution, A.A., Suranin, A.H., Taib, N.A., Mukhtar, W.M., Dasuki, K.A. and Ehsan, A.A. (2017) Chemical tapering of polymer optical fiber. *In EPJ Web of Conferences*, 162, p. 01015.

- Rashid, A.R.A., Shamsuri, N.A.F., Surani, A.H., Hakim, A.A.N. and Ismail, K. (2019) Zinc oxide coated polymer optical fiber for measuring uric acid concentrations. *Optoelectronics and Advanced Materials-Rapid Communications*, 13(1-2), pp.63-68.
- Ravindra, N.M. and Srivastava, V.K. (1979) Variation of electronic polarizability with energy gap in compound semiconductors. *Infrared Physics*, 19(5), pp.605-606.
- Razzaq, A., Zainuddin, H., Hanaffi, F. and Chyad, R.M. (2019) Transformer oil diagnostic by using an optical fibre system: a review. *IET Science, Measurement & Technology*, 13(5), pp.615-621.
- Razzaq, A., Zainuddin, H., Hanaffi, F., Chyad, R.M., Abdul Razak, H. and Latiff, A.A. (2020) Measurement of ester based transformer oil aging using tapered single mode-multimode-single mode fiber structure. *Microwave and Optical Technology Letters*, 62(2), pp.559-564.
- Redding, B. and Cao, H. (2012) Using a multimode fiber as a high-resolution, low-loss spectrometer. *Optics letters*, 37(16), pp.3384-3386.
- Reddy, R.R. and Ahammed, Y.N. (1995) A study on the Moss relation. *Infrared physics & technology*, 36(5), pp.825-830.
- Reddy, R.R., Anjaneyulu, S. and Sarma, C.L.N. (1993) Relationship between energy gap, refractive index, bond energy and the szigeti charge in polyatomic binary compounds and semiconductors. *Journal of Physics and Chemistry of Solids*, 54(5), pp.635-637.
- Reddy, R.R., Gopal, K.R., Narasimhulu, K., Reddy, L.S.S., Kumar, K.R., Balakrishnaiah, G. and Kumar, M.R. (2009) Interrelationship between structural, optical, electronic and elastic properties of materials. *Journal of alloys and compounds*, 473(1-2), pp.28-35.
- Rifat, A.A., Ahmed, R. and Bhowmik, B.B. (2019) SOI Waveguide-Based Biochemical Sensors. In *Computational Photonic Sensors* (pp. 423-448). Springer, Cham.
- Rifat, A.A., Ahmed, R., Yetisen, A.K., Butt, H., Sabouri, A., Mahdiraji, G.A., Yun, S.H. and Adikan, F.M. (2017) Photonic crystal fiber based plasmonic sensors. *Sensors and Actuators B: Chemical*, 243, pp.311-325.

- Rivero, P.J., Goicoechea, J. and Arregui, F.J. (2018) Optical fiber sensors based on polymeric sensitive coatings. *Polymers*, 10(3), p.280.
- Rivero, P.J., Urrutia, A., Goicoechea, J. and Arregui, F.J. (2012) Optical fiber humidity sensors based on Localized Surface Plasmon Resonance (LSPR) and Lossy-mode resonance (LMR) in overlays loaded with silver nanoparticles. *Sensors and Actuators B: Chemical*, 173, pp.244-249.
- Rodrigo, S.G., García-Vidal, F.J. and Martín-Moreno, L. (2008) Influence of material properties on extraordinary optical transmission through hole arrays. *Physical Review B*, 77(7), p.075401.
- Rohrbach, A. (2000) Observing secretory granules with a multiangle evanescent wave microscope. *Biophysical journal*, 78(5), pp.2641-2654.
- Rose, J.H., Ferrante, J. and Smith, J.R. (1981) Universal binding energy curves for metals and bimetallic interfaces. *Physical Review Letters*, 47(9), p.675.
- Sadiku, M.N. *Optical and wireless communications: next generation networks*. CRC press: Taylor and Francis. 2018.
- Sagadevan, S., Vennila, S., Lett, J.A., Marlinda, A.R., Hamizi, N.A.B. and Johan, M.R. (2019) Tailoring the structural, morphological, optical, thermal and dielectric characteristics of ZnO nanoparticles using starch as a capping agent. *Results in Physics*, 15, p.102543.
- Sattarin, M., Modarresi, H., Bayat, M. and Teymori, M. (2007) New viscosity correlations for dead crude oils. *Petroleum & Coal*, 49(2), pp.33-39.
- Sattler, K.D. *21st Century Nanoscience—A Handbook: Design Strategies for Synthesis and Fabrication* (Volume Two). CRC Press: Taylor and Francis. 2019.
- Schieber, M. (1991) Deposition of high temperature superconducting films by physical and chemical methods. *Journal of crystal growth*, 109(1-4), pp.401-417.
- Semwal, V. and Gupta, B.D. (2017) LSPR-and SPR-based fiber-optic cholesterol sensor using immobilization of cholesterol oxidase over silver nanoparticles coated graphene oxide nanosheets. *IEEE Sensors Journal*, 18(3), pp.1039-1046.

- Sequeira, F., Cennamo, N., Rudnitskaya, A., Nogueira, R., Zeni, L. and Bilro, L. (2019) D-Shaped POF Sensors for Refractive Index Sensing—The Importance of Surface Roughness. *Sensors*, 19(11), p.2476.
- Sharma, N., Joy, A., Mishra, A.K. and Verma, R.K. (2015) Fuchs Sondheimer–Drude Lorentz model and Drude model in the study of SPR based optical sensors: A theoretical study. *Optics Communications*, 357, pp.120-126.
- Sharma, N.K. (2012) Performances of different metals in optical fibre-based surface plasmon resonance sensor. *Pramana*, 78(3), pp.417-427.
- Shen, L., Ji, J. and Shen, J. (2008) Silver mirror reaction as an approach to construct superhydrophobic surfaces with high reflectivity. *Langmuir*, 24(18), pp.9962-9965.
- Shi, L., Chen, X., Liu, H., Chen, Y., Ye, Z., Liao, W. and Xia, Y. (2006) Fabrication of submicron-diameter silica fibers using electric strip heater. *Optics express*, 14(12), pp.5055-5060.
- Shibata, M., Sakai, Y. and Yokoyama, D. (2015) Advantages and disadvantages of vacuum-deposited and spin-coated amorphous organic semiconductor films for organic light-emitting diodes. *Journal of Materials Chemistry C*, 3(42), pp.11178-11191.
- Shobin, L.R., Sastikumar, D. and Manivannan, S. (2014) Glycerol mediated synthesis of silver nanowires for room temperature ammonia vapor sensing. *Sensors and Actuators A: Physical*, 214, pp.74-80.
- Singh, S.K., Dutta, D., Das, S., Dhar, A. and Paul, M.C. (2020) Synthetic and structural investigation of ZnO nano-rods, hydrothermally grown over Au coated optical fiber for evanescent field-based detection of aqueous ammonia. *Materials Science in Semiconductor Processing*, 107, p.104819.
- Subashini, T., Renganathan, B., Stephen, A. and Prakash, T. (2018) Acetone sensing behaviour of optical fiber clad-modified with γ -CuBr nanocrystals. *Materials Science in Semiconductor Processing*, 88, pp.181-185.
- Sulaiman, N.H., Razak, H.A., Haroon, H., Zain, A.S.M. and Fadzullah, S.H.S.M. (2019) January. Sensitivity enhancement of singlemode-multimode-singlemode fiber optic sensor based on macrobending effect for food composition monitoring. *In Journal of Physics: Conference Series* (Vol. 1151, No. 1, p. 012026). IOP Publishing.

- Supian, L.S., Ab-Rahman, M.S. and Arsad, N. (2017) Polymer optical fiber tapering using chemical solvent and polishing. *In EPJ Web of Conferences* (Vol. 162, p. 01018). EDP Sciences.
- Sypabekova, M., Korganbayev, S., González-Vila, Á., Caucheteur, C., Shaimerdenova, M., Ayupova, T., Bekmurzayeva, A., Vangelista, L. and Tosi, D. (2019) Functionalized etched tilted fiber Bragg grating aptasensor for label-free protein detection. *Biosensors and Bioelectronics*, 146, p.111765.
- Taborda, E.A., Franco, C.A., Lopera, S.H., Alvarado, V. and Cortés, F.B. (2016) Effect of nanoparticles/nanofluids on the rheology of heavy crude oil and its mobility on porous media at reservoir conditions. *Fuel*, 184, pp.222-232.
- Takimoto, B., Nabika, H. and Murakoshi, K. (2009) Enhanced Emission from Photoactivated Silver Clusters Coupled with Localized Surface Plasmon Resonance. *The Journal of Physical Chemistry C*, 113(27), pp.11751-11755.
- Tan, F.S., Sugihara, O. and Kaino, T. (2010) Encircled flux-based optimized simple launch condition for standardization of multimode polymer optical waveguide evaluations. *Optics Express*, 18(23), pp.23554-23561.
- Tang, M., Wu, Y., Deng, D., Wei, J., Zhang, J., Yang, D. and Li, G. (2018) Development of an optical fiber immunosensor for the rapid and sensitive detection of phthalate esters. *Sensors and Actuators B: Chemical*, 258, pp.304-312.
- Tang, X. and Yan, X. (2017) Dip-coating for fibrous materials: mechanism, methods and applications. *Journal of Sol-Gel Science and Technology*, 81(2), pp.378-404.
- Taylor, S.D., Czarnecki, J. and Masliyah, J. (2001) Refractive index measurements of diluted bitumen solutions. *Fuel*, 80(14), pp.2013-2018.
- Teng, F., Zheng, L., Hu, K., Chen, H., Li, Y., Zhang, Z. and Fang, X. (2016) A surface oxide thin layer of copper nanowires enhanced the UV selective response of a ZnO film photodetector. *Journal of Materials Chemistry C*, 4(36), pp.8416-8421.
- Thapa, D., Huso, J., Morrison, J.L., Corolewski, C.D., McCluskey, M.D. and Bergman, L. (2016) Achieving highly-enhanced UV photoluminescence and its origin in ZnO nanocrystalline films. *Optical Materials*, 58, pp.382-389.

- Tiede, K., Boxall, A.B., Tear, S.P., Lewis, J., David, H. and Hassellöv, M. (2008) Detection and characterization of engineered nanoparticles in food and the environment. *Food Additives and Contaminants*, 25(7), pp.795-821.
- Tripathy, S.K. and Pattanaik, A. (2016) Optical and electronic properties of some semiconductors from energy gaps. *Optical Materials*, 53, pp.123-133.
- Turcotte, R., Schmidt, C.C., Emptage, N.J. and Booth, M.J. (2019) Focusing light in biological tissue through a multimode optical fiber: refractive index matching. *Optics letters*, 44(10), pp.2386-2389.
- Urrutia, A., Del Villar, I., Zubieta, P. and Zamarreño, C.R. (2019) A Comprehensive Review of Optical Fiber Refractometers: Toward a Standard Comparative Criterion. *Laser & Photonics Reviews*, 13(11), p.1900094.
- Usha, S.P., Mishra, S.K. and Gupta, B.D. (2015) Fabrication and characterization of a SPR based fiber optic sensor for the detection of chlorine gas using silver and zinc oxide. *Materials*, 8(5), pp.2204-2216.
- Wan, J., Lu, Y., Li, X., Zhang, Z., Yang, J., Jiang, G. and Hu, F. (2017) Liquid prism based refractometer. *Journal of Optics*, 19(5), p.055705.
- Wang, B. and Mies, E. (2009) February. Review of fabrication techniques for fused fiber components for fiber lasers. In *Fiber Lasers VI: Technology, Systems, and Applications* (Vol. 7195, p. 71950A). International Society for Optics and Photonics.
- Wang, P., Brambilla, G., Ding, M., Semenova, Y., Wu, Q. and Farrell, G. (2011) High-sensitivity, evanescent field refractometric sensor based on a tapered, multimode fiber interference. *Optics letters*, 36(12), pp.2233-2235.
- Wang, P., Zhao, H., Wang, X., Farrell, G. and Brambilla, G. (2018) A review of multimode interference in tapered optical fibers and related applications. *Sensors*, 18(3), p.858.
- Wang, Q., Kong, L., Dang, Y., Xia, F., Zhang, Y., Zhao, Y., Hu, H. and Li, J. (2016). High sensitivity refractive index sensor based on splicing points tapered SMF-PCF-SMF structure Mach-Zehnder mode interferometer. *Sensors and Actuators B: Chemical*, 225, pp.213-220.
- Wang, Q. and Liu, Y. (2018) Review of optical fiber bending/curvature sensor. *Measurement*, 130, pp.161-176.

- Wang, R. and Yu, G. (2019) Suspended sediment concentration measurement based on optical fiber technology. *Measurement Science and Technology*, 30(7), p.075205.
- Wang, Z.L. (2004) Nanostructures of zinc oxide. *Materials today*, 7(6), pp.26-33.
- Weber, V.L. (2017) Use of the phenomenon of total internal light reflection for diagnostics of sea wind waves. *Radiophysics and Quantum Electronics*, pp.1-10.
- Wendeln, C., Stamp, L., Dosse, B., Wurdinger, K., Krilles, G. and Nguyen, T.C.L. Process for depositing a metal or metal alloy on a surface of a substrate including its activation. U.S. *Patent Application* 16/092,459. 2019.
- Winzer, P.J., Neilson, D.T. and Chraplyvy, A.R. (2018) Fiber-optic transmission and networking: the previous 20 and the next 20 years. *Optics express*, 26(18), pp.24190-24239.
- Wolfbeis, O.S. and Weidgans, B.M. (2006) Fiber optic chemical sensors and biosensors: A view back. In *Optical chemical sensors* (pp. 17-44). Springer, Dordrecht.
- Woliński, T.R. (2015) Polarization phenomena in optical systems. In *Encyclopedia of Optical and Photonic Engineering* (Print)-Five Volume Set (pp. 1-24). CRC Press.
- Wu, Y., Deng, X., Li, F. and Zhuang, X. (2007) Less-mode optic fiber evanescent wave absorbing sensor: Parameter design for high sensitivity liquid detection. *Sensors and Actuators B: Chemical*, 122(1), pp.127-133.
- Wu, Y., Xia, L. and Cai, N. (2018) Dual-wavelength intensity-modulated Fabry–Perot refractive index sensor driven by temperature fluctuation. *Optics letters*, 43(17), pp.4200-4203.
- Yamamoto, N., Nakano, M. and Suzuki, T. (2006) Light emission by surface plasmons on nanostructures of metal surfaces induced by high-energy electron beams. *Surface and Interface Analysis*, 38(12-13), pp.1725-1730.
- Yang, H., Yu, B., Song, P., Maluk, C. and Wang, H. (2019) Surface-coating engineering for flame retardant flexible polyurethane foams: A critical review. *Composites Part B: Engineering*, 176, p.107185.

- Yap, S.H.K., Chan, K.K., Zhang, G., Tjin, S.C. and Yong, K.T. (2019) Carbon Dot-functionalized Interferometric Optical Fiber Sensor for Detection of Ferric Ions in Biological Samples. *ACS applied materials & interfaces*, 11(31), pp.28546-28553.
- Yasli, A. and Ademgil, H. (2019) Effect of plasmonic materials on photonic crystal fiber based surface plasmon resonance sensors. *Modern Physics Letters B*, 33(13), p.1950157.
- Young, S.J., Liu, Y.H. and Chien, J.T. (2018) Improving field electron emission properties of ZnO nanosheets with Ag nanoparticles adsorbed by photochemical method. *ACS omega*, 3(7), pp.8135-8140.
- Younus, M.H., Ameen, O.F., Redzuan, N., Ahmad, N. and Ibrahim, R.K.R. (2018) Fabrication and characterization of multimode optical fiber sensor for chemical temperature monitoring using optical time domain reflectometer. *Karbala International Journal of Modern Science*, 4(1), pp.119-125.
- Zaca-Morán, P., Padilla-Martínez, J.P., Pérez-Corte, J.M., Dávila-Pintle, J.A., Ortega-Mendoza, J.G. and Morales, N. (2018) Etched optical fiber for measuring concentration and refractive index of sucrose solutions by evanescent waves. *Laser Physics*, 28(11), p.116002.
- Zaca-Morán, P., Padilla-Martínez, J.P., Pérez-Corte, J.M., Dávila-Pintle, J.A., Ortega-Mendoza, J.G. and Morales, N. (2018) Etched optical fiber for measuring concentration and refractive index of sucrose solutions by evanescent waves. *Laser Physics*, 28(11), p.116002.
- Zain, H.A., Jali, M.H., Rahim, H.R.A., Johari, M.A.M., Yusof, H.H.M., Thokchom, S., Yasin, M. and Harun, S.W. (2020) ZnO nanorods coated microfiber loop resonator for relative humidity sensing. *Optical Fiber Technology*, 54, p.102080.
- Zakaria, R., Sheng, O.Y., Wern, K., Shamshirband, S., Petković, D. and Pavlović, N.T. (2014) Adaptive neuro-fuzzy evaluation of the tapered plastic multimode fiber-based sensor performance with and without silver thin film for different concentrations of calcium hypochlorite. *IEEE Sensors Journal*, 14(10), pp.3579-3584.

- Zallen, R. *The formation of amorphous solids*. The physics of amorphous solids. New York: Wiley, pp.1-22. 1983.
- Zhang, C., Ning, T., Li, J., Pei, L., Li, C. and Lin, H. (2017) Refractive index sensor based on tapered multicore fiber. *Optical Fiber Technology*, 33, pp.71-76.
- Zhang, E.J., Sacher, W.D. and Poon, J.K. (2010) Hydrofluoric acid flow etching of low-loss subwavelength-diameter biconical fiber tapers. *Optics express*, 18(21), pp.22593-22598.
- Zhang, M., Zhu, G., Li, T., Lou, X. and Zhu, L. (2020) A dual-channel optical fiber sensor based on surface plasmon resonance for heavy metal ions detection in contaminated water. *Optics Communications*, 462, p.124750.
- Zhao, Y., Wang, D., Guo, X. and Xu, J. (1998) A new spectrum technique based on direct detection of light intensity absorbed. *Science in China Series B: Chemistry*, 41(3), pp.239-246.
- Zhao, Y., Zhao, H., Lv, R.Q. and Zhao, J. (2019) Review of optical fiber Mach–Zehnder interferometers with micro-cavity fabricated by femtosecond laser and sensing applications. *Optics and Lasers in Engineering*, 117, pp.7-20.
- Zheng, B., Wong, L.P., Wu, L.Y. and Chen, Z. (2017) Identifying key factors towards highly reflective silver coatings. *Advances in Materials Science and Engineering*, 2017.
- Zheng, Y., Zhu, Z.W., Xiao, W. and Deng, Q.X. (2020) Review of fiber optic sensors in geotechnical health monitoring. *Optical Fiber Technology*, 54, p.102127.
- Zhu, X., Wang, R., Xia, K., Zhou, X. and Shi, H. (2019) Nucleic acid functionalized fiber optic probes for sensing in evanescent wave: optimization and application. *RSC advances*, 9(4), pp.2316-2324.
- Zhuang, Q., Zou, D., You, G., Li, K., Zhen, H. and Ling, Q. (2019) Solution-processed, top-emitting, microcavity polymer light-emitting diodes for the pure red, green, blue and near white emission. *Nanotechnology*, 31(8), p.085201.
- Zhuang, X.Y., Wu, Y.H., Wang, S.R. and Xuan, M. (2008) Optical fiber evanescent field sensor based on new type D-shaped fiber. *Opt. Precision Eng.*, 16, pp.1936-1941.

- Zink, J., Wyrobnik, T., Prinz, T. and Schmid, M. (2016) Physical, chemical and biochemical modifications of protein-based films and coatings: An extensive review. *International journal of molecular sciences*, 17(9), p.1376.
- Zinth, W., Laubereau, A. and Kaiser, W. (2011) The long journey to the laser and its rapid development after 1960. *The European Physical Journal H*, 36(2), pp.153-181.
- Zu, L., Zhang, H., Fei, C., Miao, Y., Li, B. and Yao, J. (2019) Highly sensitive chloride ion concentration measurement based on a multitaper modulated fiber. *Optical Engineering*, 58(8), p.086109.

LIST OF PUBLICATIONS

Journal with Impact Factor

1. **Samavati, Z.**, Samavati, A., Ismail, A.F., Yahya, N., Rahman, M.A. and Othman, M.H.D. (2020). Effect of acetone/methanol ratio as a hybrid solvent on fabrication of polymethylmethacrylate optical fiber sensor. *Optics & Laser Technology*, 123, p.105896. **(Q1, IF: 3.323)**
2. **Samavati, Z.**, Samavati, A., Ismail, A.F., Yahya, N., Othman, M.H.D. and Rahman, M.A. (2020). Modified polymer optical fiber sensors for crude oil refractive index monitoring. *Journal of Materials Science: Materials in Electronics*, pp.1-12. **(Q2, IF: 2.220)**
3. **Samavati, Z.**, Samavati, A., Ismail, A.F., Yahya, N., Othman, M.H.D., Rahman, M.A., Bakar, M.A.A. and Amiri, I.S. (2020). The impact of ZnO configuration as an external layer on the sensitivity of a bi-layer coated polymer optical fiber probe. *RSC Advances*, 10(22), pp.12864-12875. **(Q2, IF: 3.119)**
4. **Samavati, Z.**, Samavati, A., Ismail, A.F., Othman, M.H.D. and Rahman, M.A. (2019). Comprehensive investigation of evanescent wave optical fiber refractive index sensor coated with ZnO nanoparticles. *Optical Fiber Technology*, 52, p.101976. **(Q2, IF: 2.212)**
5. **Samavati, Z.**, Samavati, A., Ismail, A.F., Rahman, M.A. and Othman, M.H.D. (2019). Detection of saline-based refractive index changes via bilayer ZnO/Ag-coated glass optical fiber sensor. *Applied Physics B*, 125(9), p. 161. **(Q3, IF: 1.817)**
6. **Samavati, Z.**, Samavati, A., Ismail, A.F., Rahman, M.A. and Othman, M.H.D. (2018). Intensity modulated silver coated glass optical fiber refractive index sensor. *Chinese Optics Letters*, 16(9), p.090602. **(Q3, IF: 2.045)**

7. Samavati, A., **Samavati, Z.**, Ismail, A.F., Yahya, N., Othman, M.H.D. and Rahman, M.A. (2020). Multi aspect investigation of crude oil concentration detecting via optical fiber sensor coated with ZnO/Ag nano-heterostructure. *Measurement*, p.108171. **(Q1, IF: 3.364)**
8. Samavati, A., **Samavati, Z.**, Ismail, A.F., Yahya, N., Bakar, M.A.A., Othman, M.H.D., Rahman, M.A., Koo, K.N. and Osman, S.S. (2019). Magnetic field detection using a highly sensitive FBG probe. *Physica Scripta*. **(Q2, IF: 1.985)**
9. Samavati, A., **Samavati, Z.**, Ismail, A.F., Yahya, N., Othman, M.H.D., Rahman, M.A., Bakar, M.A.A., Koo, K.N., Salebi, M.F. and Amiri, I.S. (2019). An FBG magnetic sensor for oil flow monitoring in sandstone core. *RSC Advances*, 9(61), pp.35878-35886. **(Q2, IF: 3.119)**
10. Samavati, A., **Samavati, Z.**, Ismail, A.F., Othman, M.H.D., Rahman, M.A. and Amiri, I.S. (2018). Effect of organic ligand-decorated ZnO nanoparticles as a cathode buffer layer on electricity conversion efficiency of an inverted solar cell. *RSC advances*, 8(3), pp.1418-1426. **(Q2, IF: 3.119)**

International Conferences

1. **Samavati, Z.**, Ismail, A.F. and Rahman, M.A. (2018). ZnO/Ag/Glass optical fiber as a sensing probe for detecting the refractive index changes. *National congress of membrane technology*. 30th-31st October 2018, Johor Bahru, Malaysia.
2. **Samavati, Z.**, Samavati, A., Ismail, A.F., Rahman, M.A. and Othman, M.H.D. (2019) Optical Fiber Refractive Index Sensor Based on Partially Unclad Multimode Fiber Coated with ZnO Nanoparticles. *International Conference of Sustainable Environmental Technology*. 20th-22nd August 2019, Johor Bahru, Malaysia.
3. **Samavati, Z.**, Samavati, A., Ismail, A.F., Yahya, N., Rahman, M.A. and Othman, M.H.D. (2019) The role of acetone concentration as etching solvent on fabrication of partially unclad polymer optical fiber sensor. *International Laser Technology and Optics Symposium 2019*. 3rd – 4th September 2019, Johor Bahru, Malaysia.

APPENDIX A

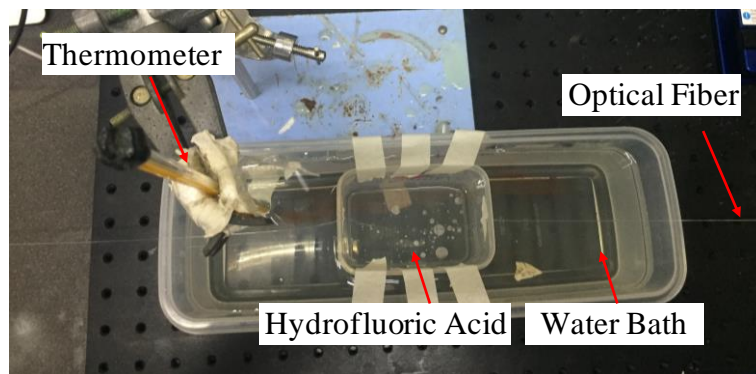
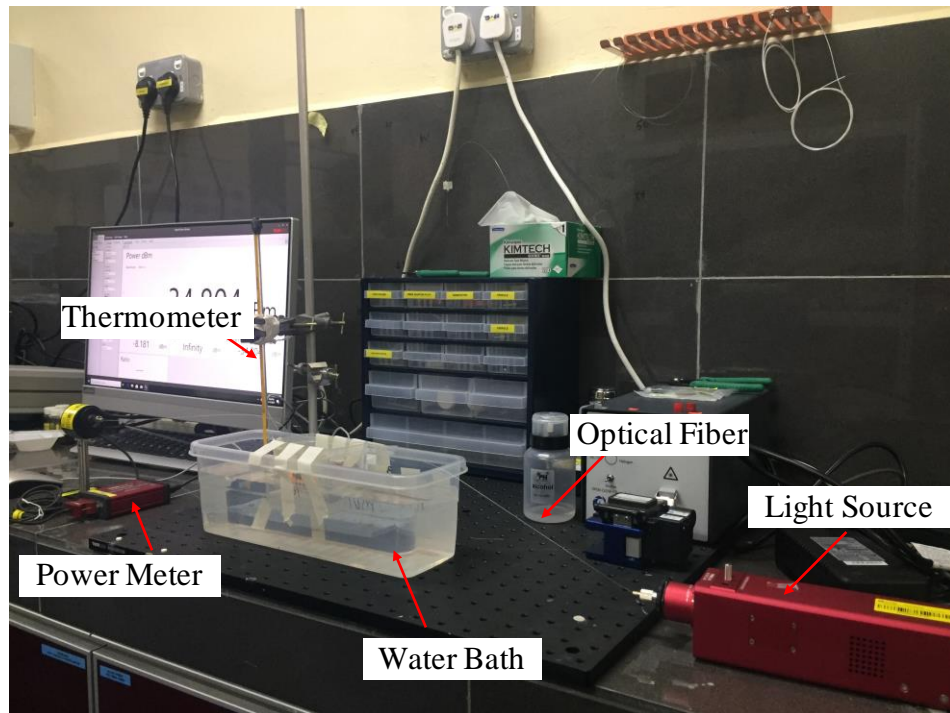


Figure A.1 Un-cladding process via etching method by varying the temperature and solvents concentrations for GOF and POF.

APPENDIX B

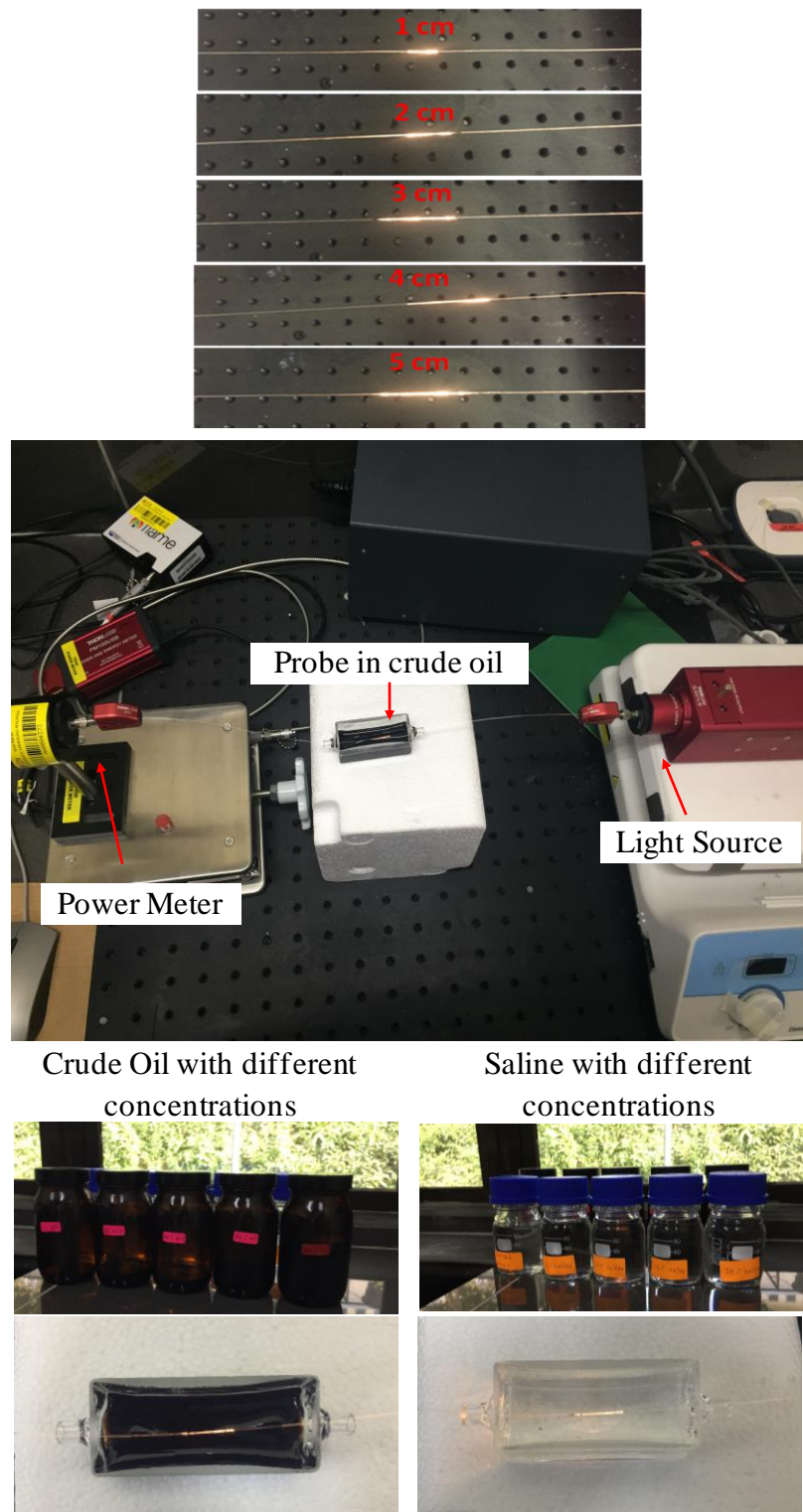


Figure B.1 performance analysis of partially unclad fiber against refractive index changes. The refractive index of saline and crude oil solutions varied from 1.333-1.368 and 1.372-1.478 respectively.

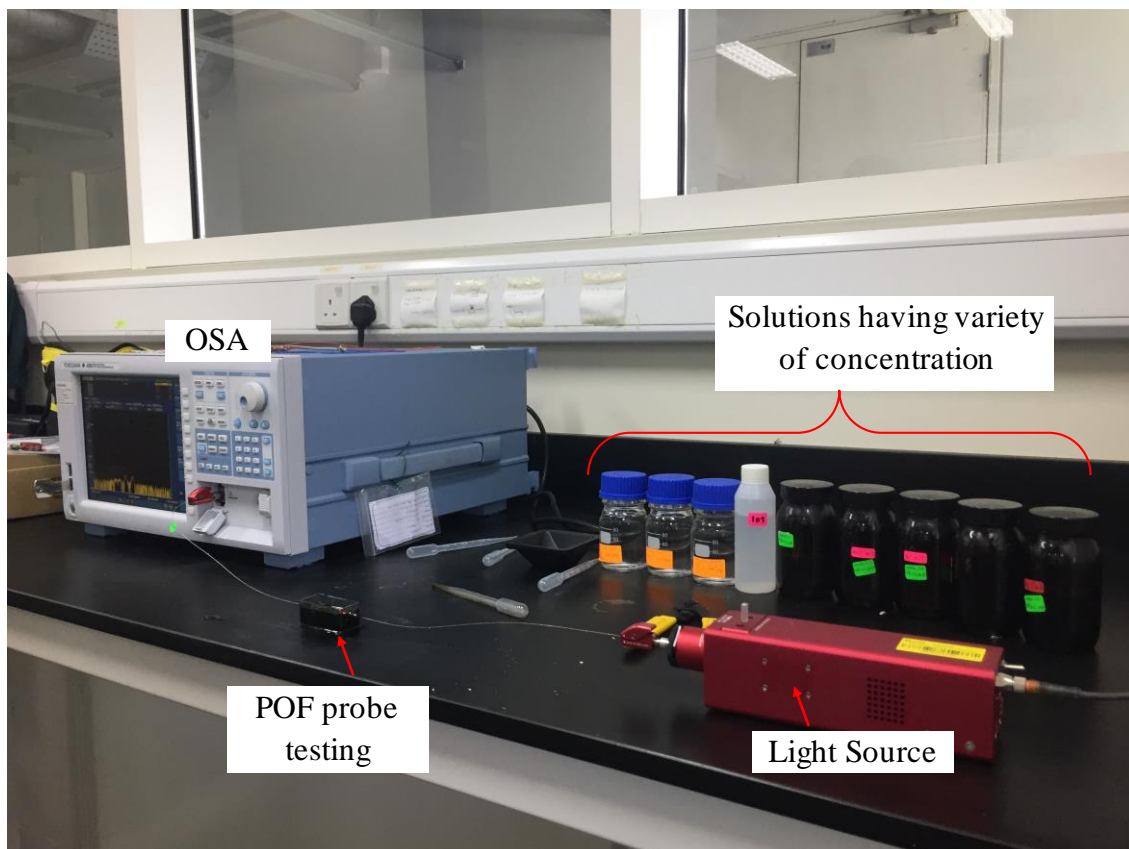


Figure B.2 performance process of probes coated with bi-layer ZnO/Ag on POF and GOF for detecting the concentration changes of saline and crude oil.